mcnp5

Diagnostics Applications Group (X-5)

Los Alamos NATIONAL LABORATORY

ANS Mathematics & Computation Topical Meeting

Avignon,France, 11–15 September 2005

LA-UR-05–5618

Advances in Monte Carlo Criticality Calculations

Forrest B. Brown & Russell D. Mosteller

X-5, Los Alamos National Laboratory

fbrown@lanl.gov, mosteller@lanl.gov

Advances in Monte Carlo Criticality Calculations

Forrest B. Brown & Russell D. Mosteller

**Diagnostics Applications Group (X-5), LANL**

This workshop will focus on recent advances in methods, codes, and data for Monte Carlo criticality calculations, including: improvements to MCNP5 kcode calculations, source entropy as a convergence diagnostic, Weilandt acceleration, stochastic geometry for HTGRs, use of mesh tallies for reactor applications, pre-ENDF/B-VII data, Doppler broadening, material composition library, etc.

Advances in Monte Carlo Criticality Calculations

- **Introduction**

- **Entropy of the Fission Source Distribution**

- **Mesh Tallies for Reactor Applications**

- **Nuclear Data for MCNP**

- **Monte Carlo Power Iteration & Weilandt Method**

- **HTGR Modeling & Stochastic Geometry**

mcnp5

**Diagnostics
Applications
Group (X-5)**

Los Alamos
NATIONAL LABORATORY

Entropy of the Fission Source Distribution & Stationarity Diagnostics

Keff Calculations

mcnp5

**Diagnostics
Applications
Group (X-5)**

Los Alamos
NATIONAL LABORATORY

- **Plots of single-cycle Keff or cumulative Keff are sometimes difficult to interpret when assessing convergence**


Cycle k_{eff}
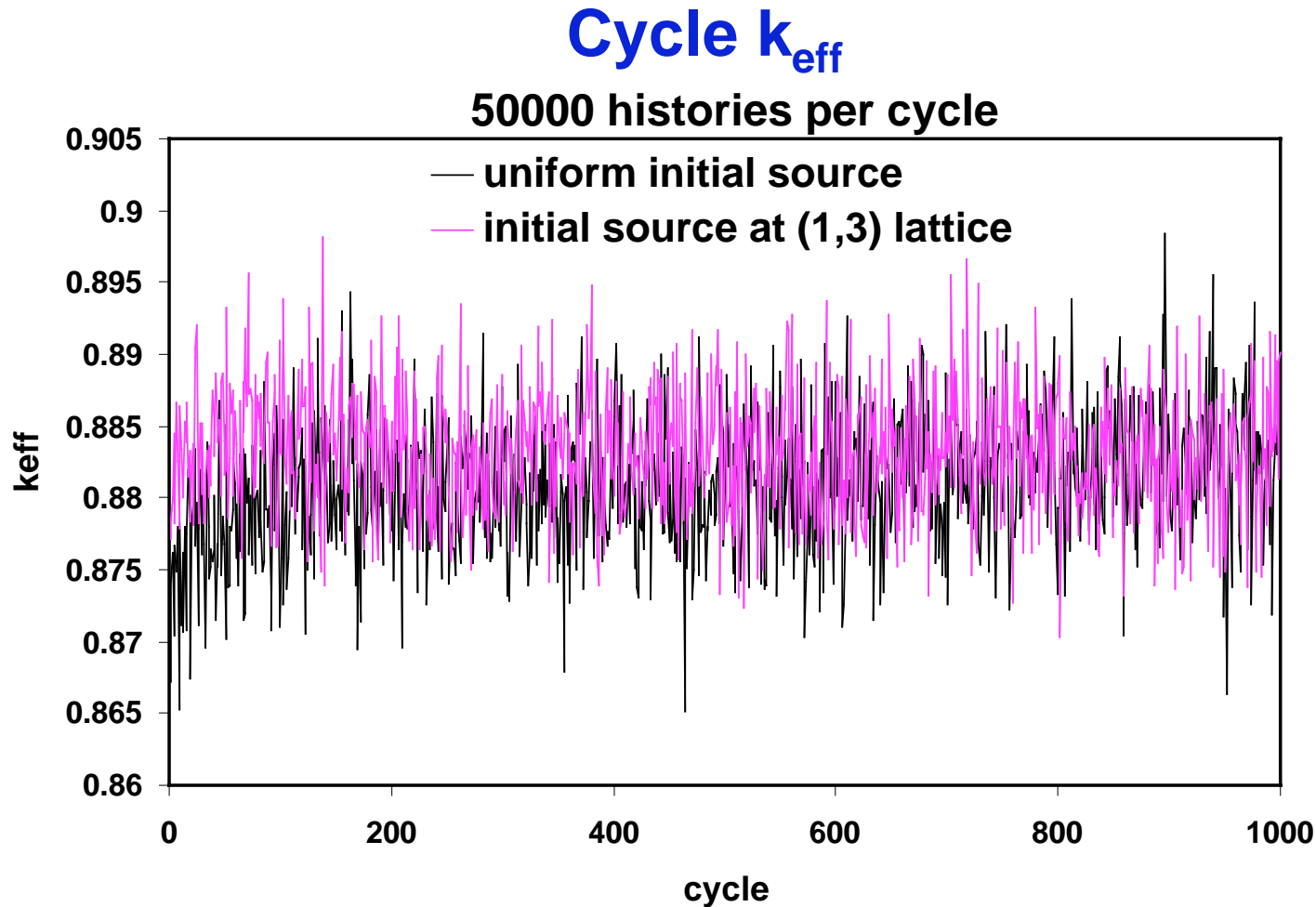
- **Initial cycles of a Monte Carlo K-effective calculation should be discarded, to avoid contaminating results with errors from initial guess**
  - **How many cycles should be discarded?**
  - **How do you know if you discarded enough cycles?**

$K_{eff}^{(n)}$

Discard   **Tallies**
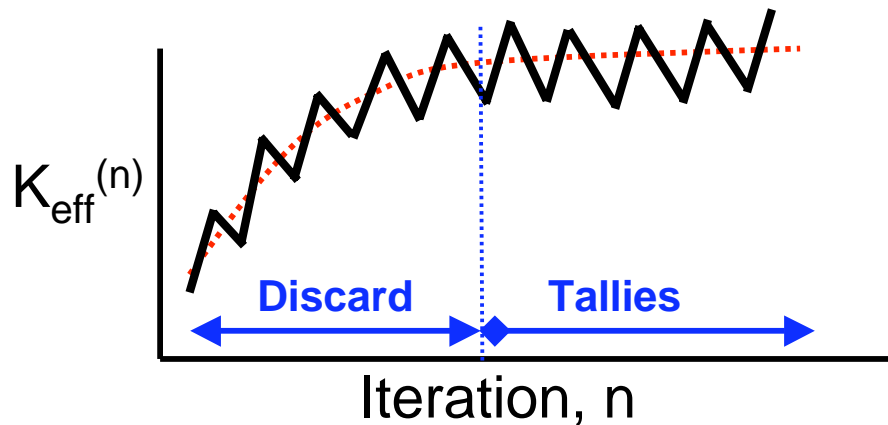
Iteration, n

- **Analysis of the power iteration method shows that Keff is not a reliable indicator of convergence** — K_{eff} can converge faster than the source shape

- **Based on concepts from information theory, Shannon entropy of the source distribution is useful for characterizing the convergence of the source distribution**

K$_{eff}$ Calculations – Stationarity Diagnostics

mcnp5

Diagnostics
Applications
Group (X-5)

Los Alamos
NATIONAL LABORATORY

- Divide the fissionable regions of the problem into **N$_S$ spatial bins**

  - Spatial bins should be consistent with problem symmetry
  - Typical choices: — 1 bin for each assembly
                      — regular grid superimposed on core
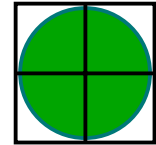
  - Rule-of-thumb for number of spatial bins:

    N$_S$ ~ (histories/batch) / 25 or less

    Why?
    - Would like to have >25 fission source sites per bin to get good statistics
    - If source distribution were uniform, ~25 sites would be in each bin

- **Shannon entropy of the source distribution**

$$H(S) = -\sum_{J=1}^{N_S} p_J \cdot \ln_2(p_J), \quad \text{where} \quad p_J = \frac{(\text{\# source particles in bin J})}{(\text{total \# source particles in all bins})}$$

- **Shannon entropy of the source distribution**

$$H(S) = -\sum_{J=1}^{N_S} p_J \cdot \ln_2(p_J), \quad \text{where} \quad p_J = \frac{(\text{\# source particles in bin } J)}{(\text{total \# source particles in all bins})}$$

  – **$0 \leq H(S) \leq \ln_2(N_S)$**

  – Note that $p_J \ln_2(p_J) = 0$ if $p_J = 0$

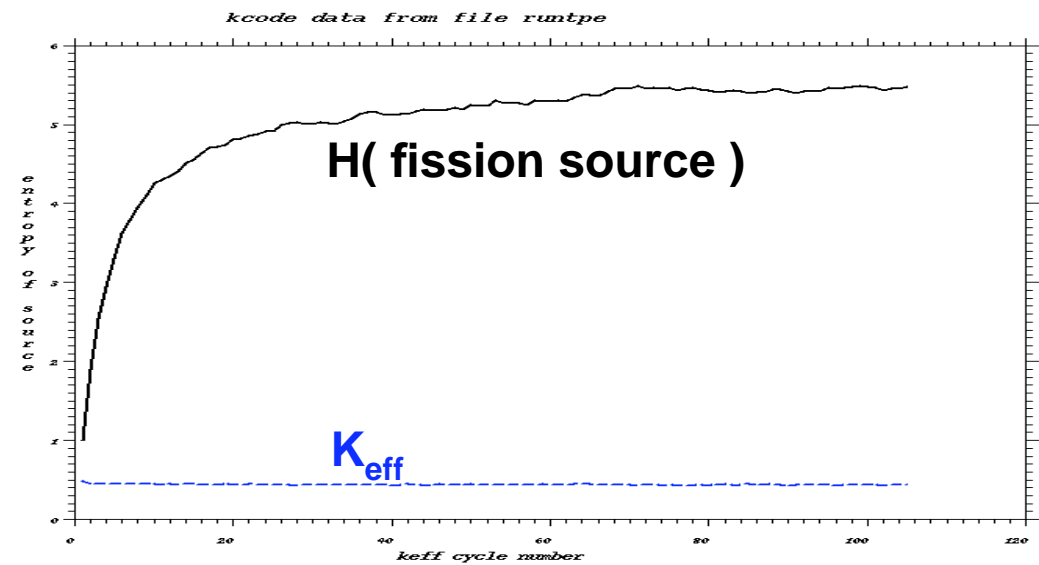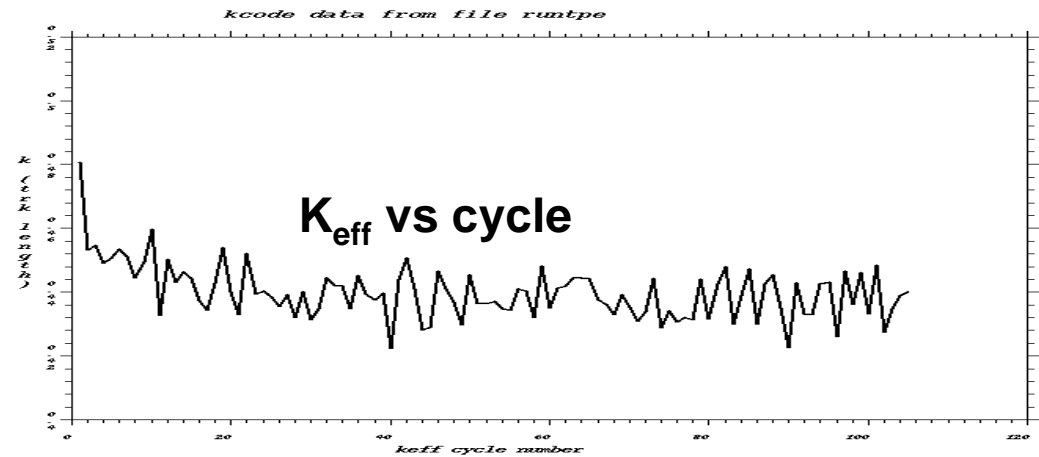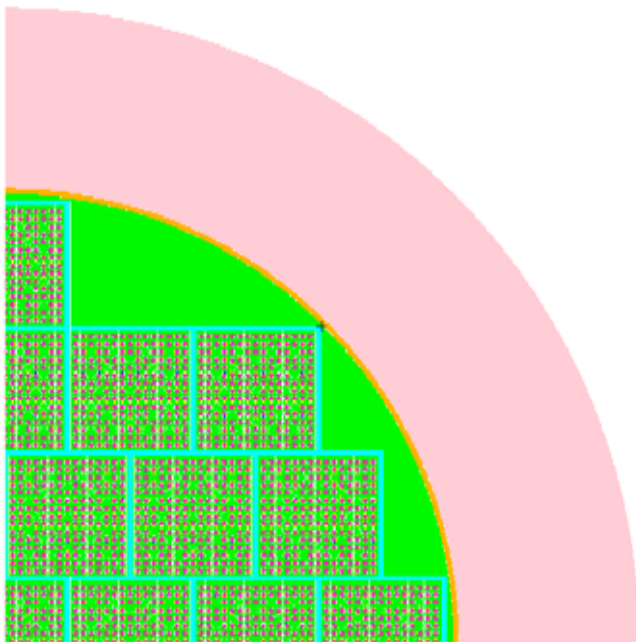 – **For a uniform source distribution,** $p_1 = p_2 = \ldots = p_{Ns} = 1/N_S$, so that **$H(S) = \ln_2(N_S)$**

  – **For a point source (in a single bin), $H(S) = 0$**

- **$H(S^{(n)})$ provides a single number to characterize the source distribution for iteration n**

  $\Rightarrow$ **As the source distribution converges in 3D space, a line plot of $H(S^{(n)})$ vs. n (the iteration number) converges**
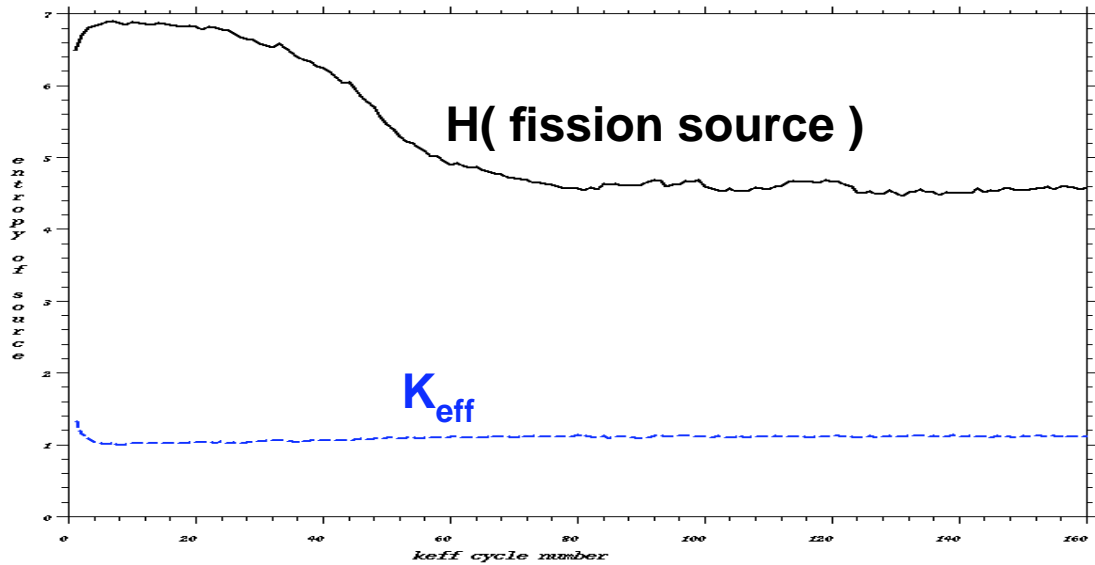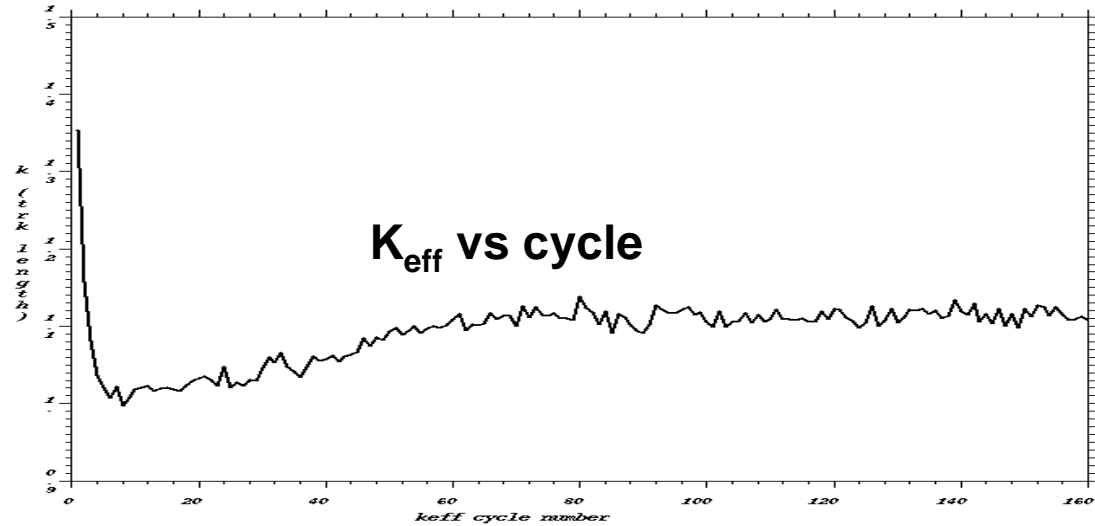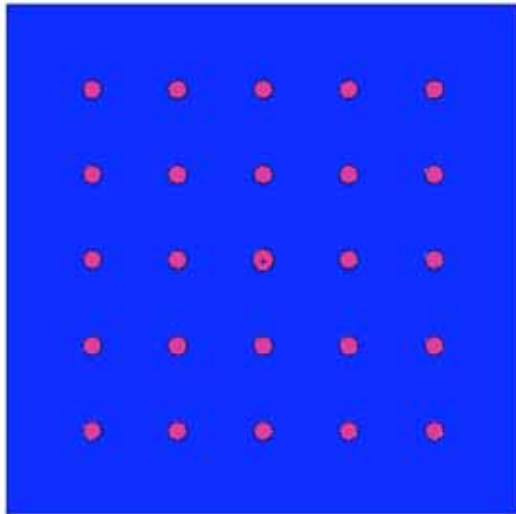
K$_{eff}$ Calculations – Stationarity Diagnostics

- **Example – Reactor core (Problem inp24)**

K$_{eff}$ vs cycle

H(fission source)

K$_{eff}$

K$_{eff}$ Calculations – Stationarity Diagnostics

mcnp5

Diagnostics
Applications
Group (X-5)

Los Alamos
NATIONAL LABORATORY

- **Example – Loosely-coupled array of spheres (Problem test4s)**

K$_{eff}$ vs cycle

H(fission source)

K$_{eff}$

K_{eff} Calculations – Stationarity Diagnostics

- **Example – Fuel Storage Vault (Problem OECD_bench1)**

K_{eff} vs cycle

H(fission source)
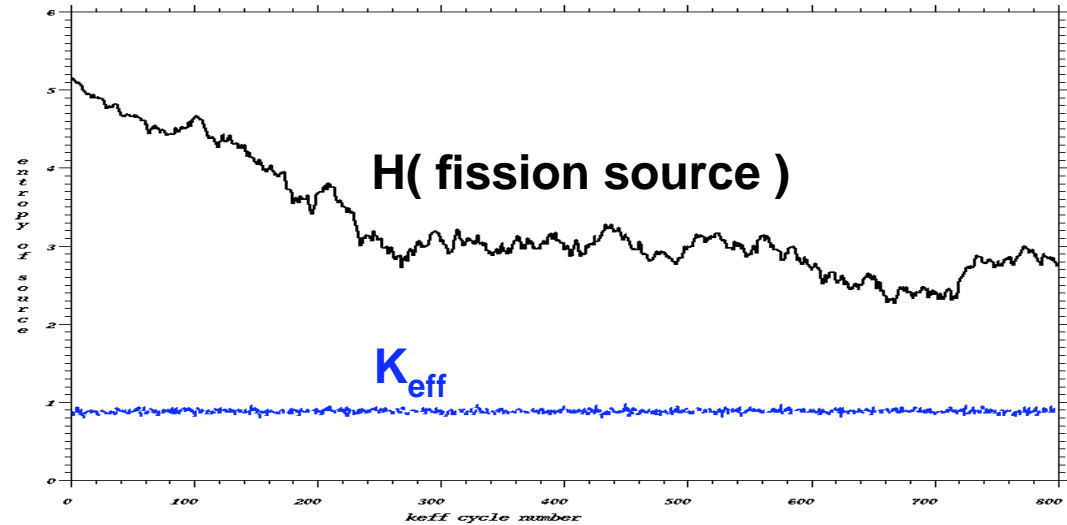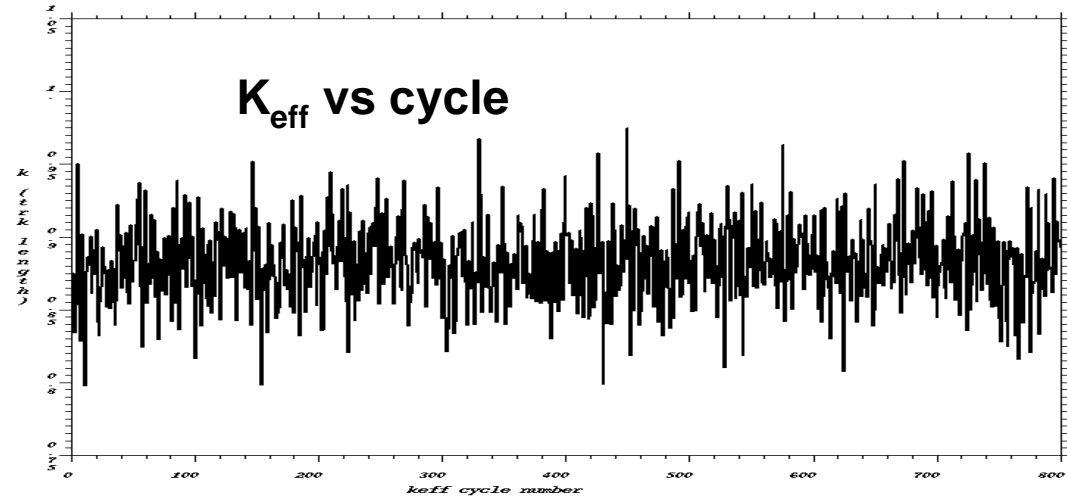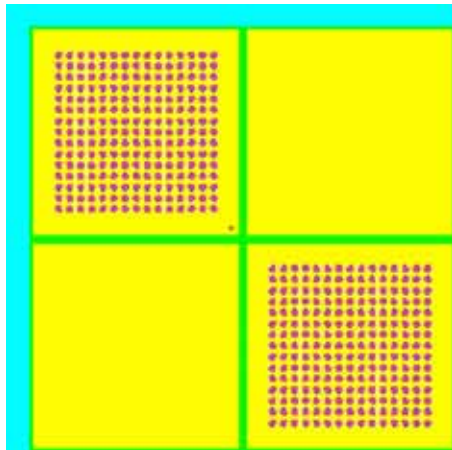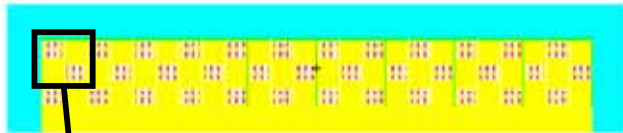
K_{eff}

- Example – PWR 1/4-Core   (Napolitano)

kcode data from file runtpf

K$_{eff}$ vs cycle

keff cycle number

kcode data from file runtpf

H(fission source)

keff cycle number

- **Example – 2D PWR (Ueki)**

kcode data from file runtpe

K_{eff} vs cycle

H(fission source)

13
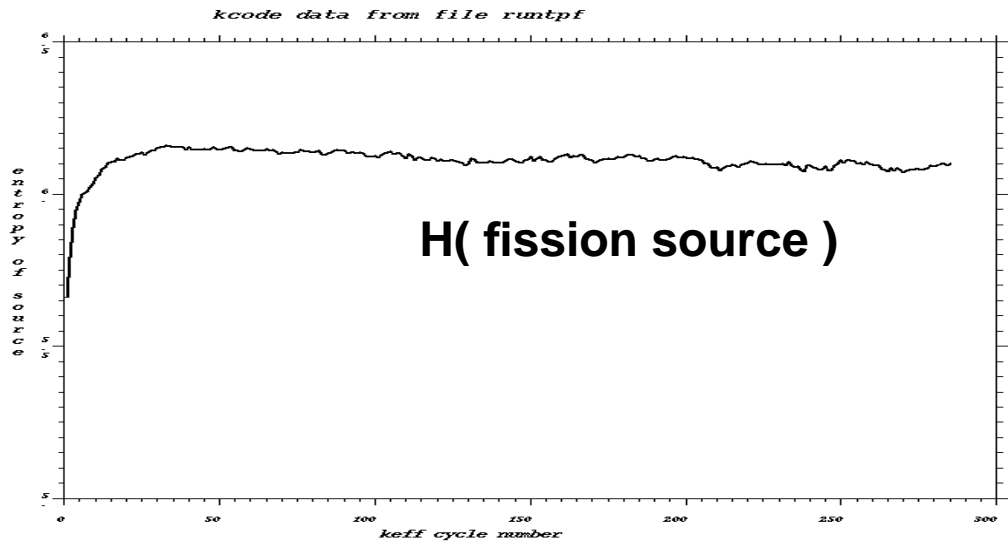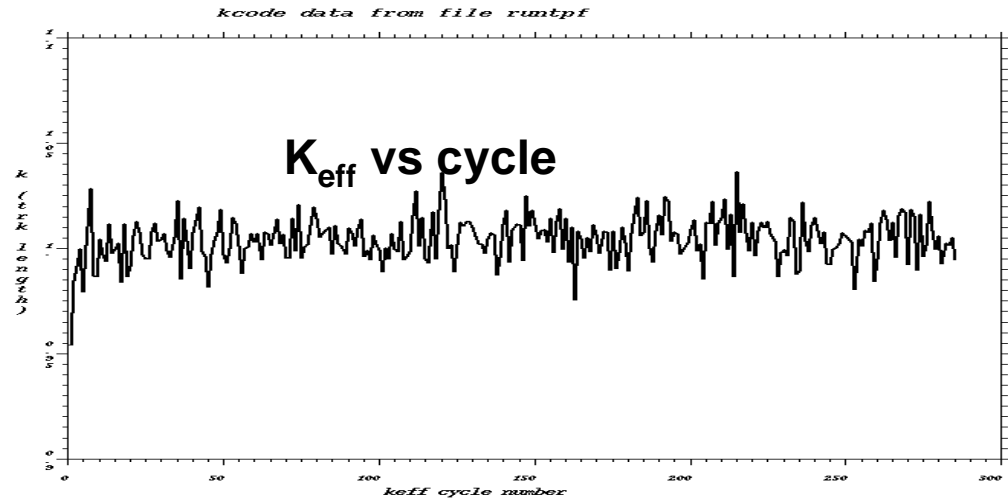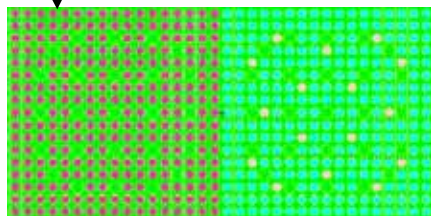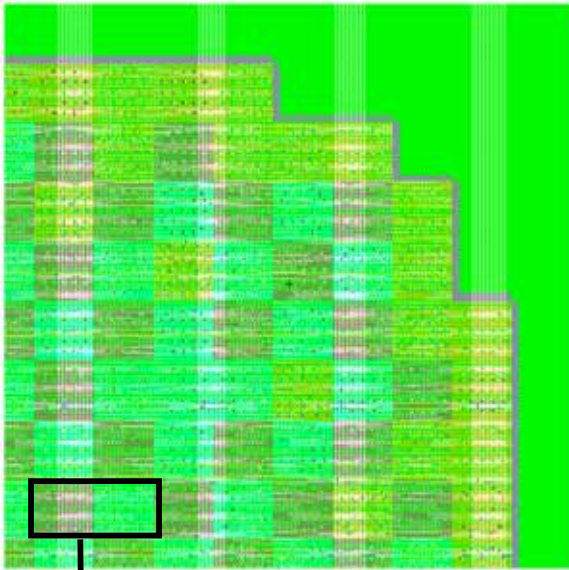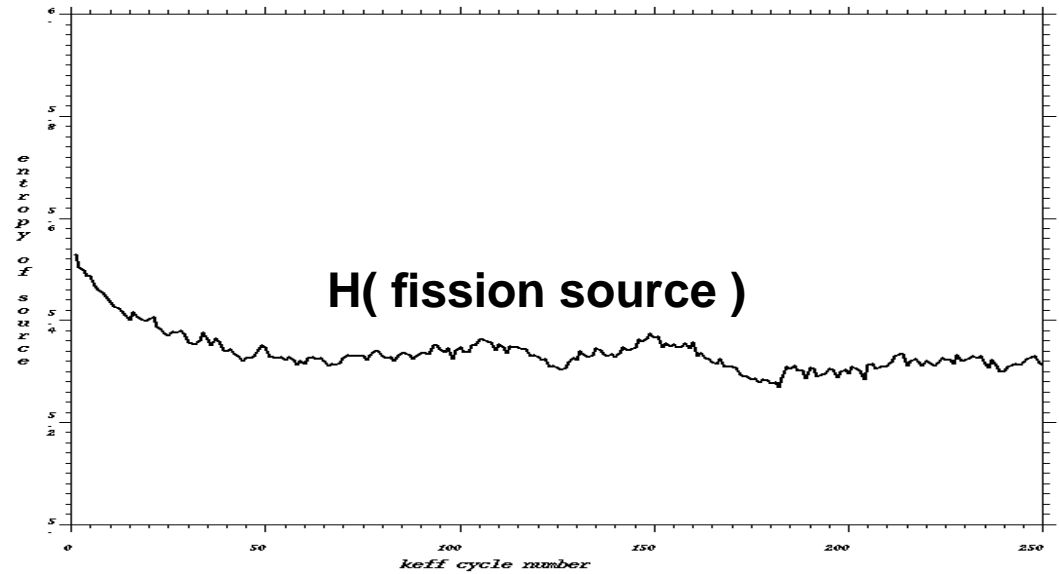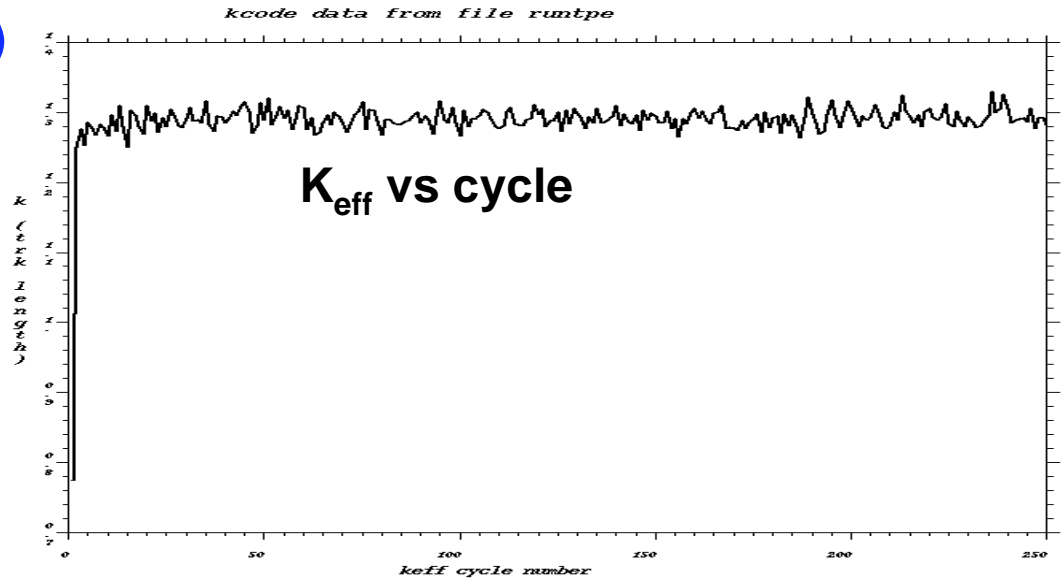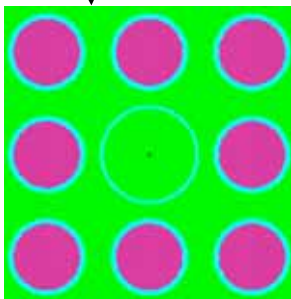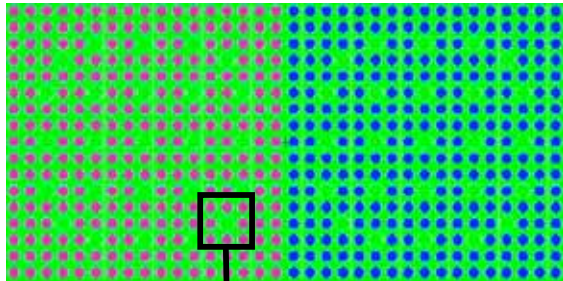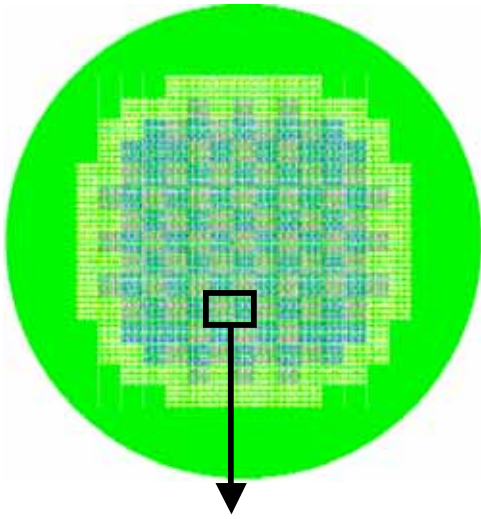
- **Grid for computing H_{src}**
  - User can specify a rectangular grid in input

    hsrc $\quad$ n_x x_{min} x_{max} $\quad\quad$ n_y y_{min} y_{max} $\quad\quad$ n_z z_{min} z_{max}

    example: $\quad\quad$ hsrc $\quad$ 5 0. 100. $\quad$ 5 0. 100. $\quad$ 1 -2. 50.

  - If hsrc card is absent, MCNP5 will choose a grid based on the fission source points, expanding it if needed during the calculation

- **MCNP5 prints H_{src} for each cycle**

- **MCNP5 can plot H_{src} vs cycle**

- **Convergence check at end of problem**
  - MCNP5 computes the average H_{src} and its population variance σ_H^2 for the last half of the cycles
  - Then, finds the first cycle where H_{src} is within the band $<H_{src}> \pm 2\sigma_H$
  - Then, checks to see if at least that many cycles were discarded

mcnp5

**Diagnostics
Applications
Group (X-5)**

Los Alamos
NATIONAL LABORATORY

Mesh Tallies
For Reactor Applications

Mesh tallies are track-length tallies that cover 3D regions of space, independent of the problem geometry
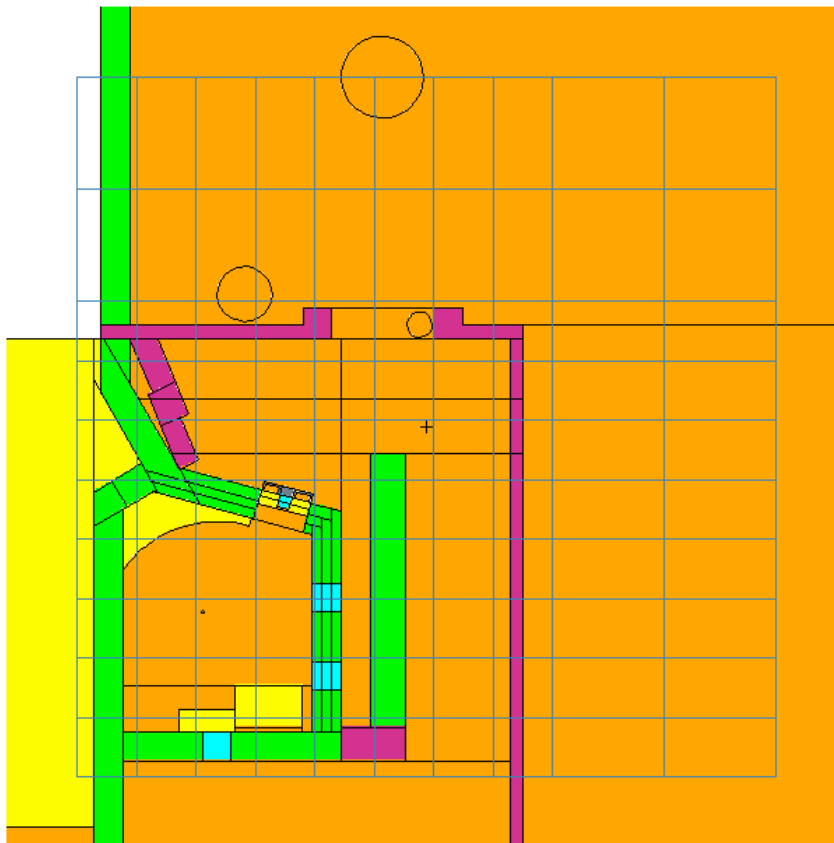
- Both rectangular and cylindrical meshes
- Bin on energy values
- Unlimited number of meshes
- Size of mesh limited by computer parameters
- Rotated by using a TR card
- Modified by DE/DF cards or an FM card
- Surface and cell flagging
- Plot results

Built-in plotter now plots mesh tally results on top of geometry outline

Proton Storage Ring
at LANSCE accelerator

Geometry

Blue = concrete

Yellow = air
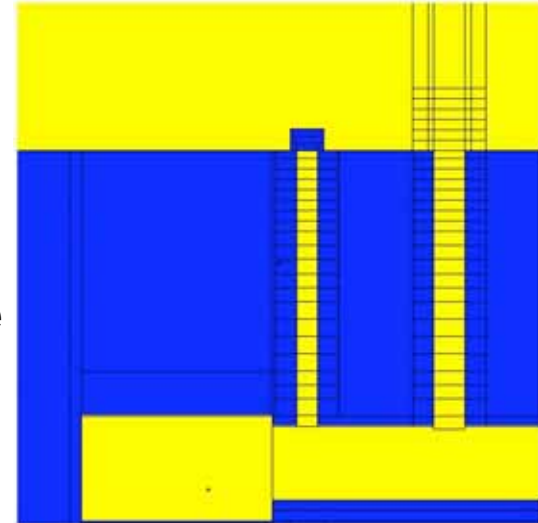
Dose rate calculation for cable penetrations
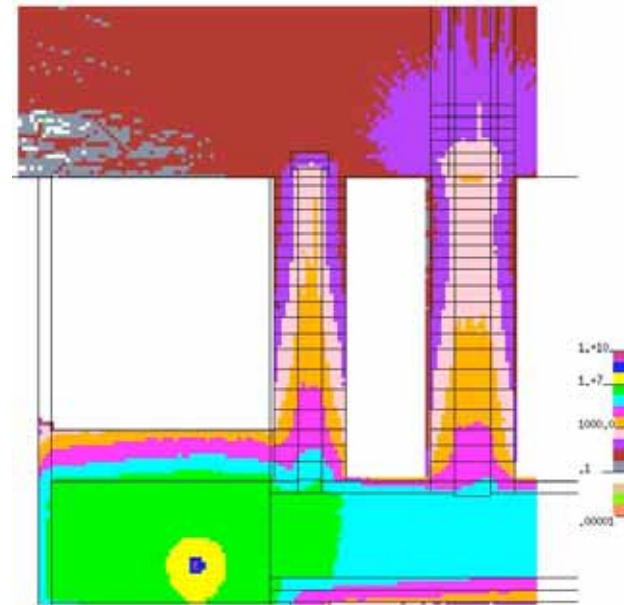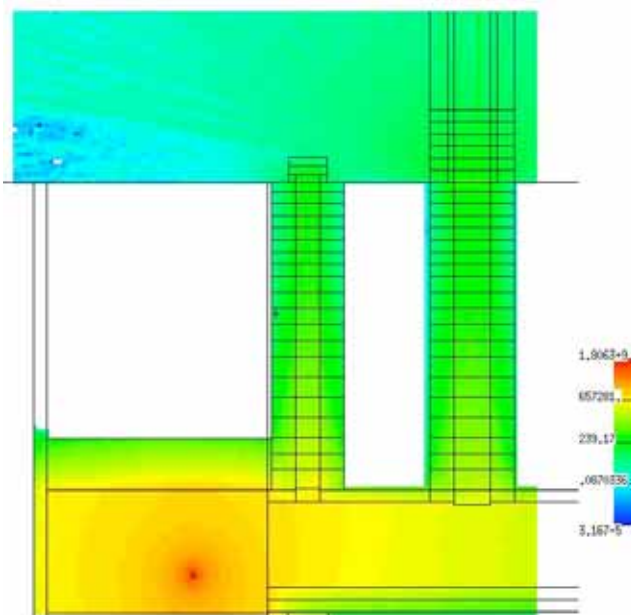
Mesh Tallies & the FM card

Some calculations, such as energy deposition, require the use of the FM card. However, the FM card requires the user to identify a material whose reaction cross sections are used in the tally. This is impractical for a tally that contains several materials.

Fuel Storage Vault
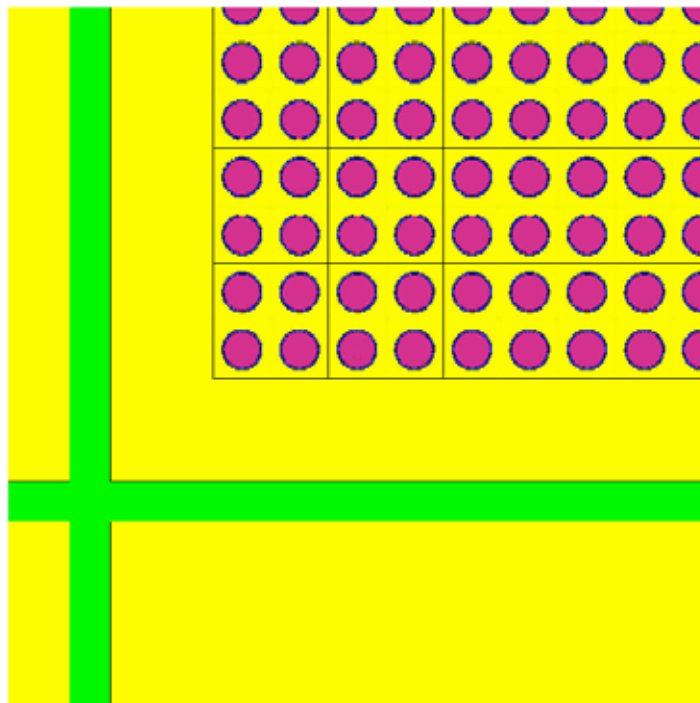
Neutron Flux
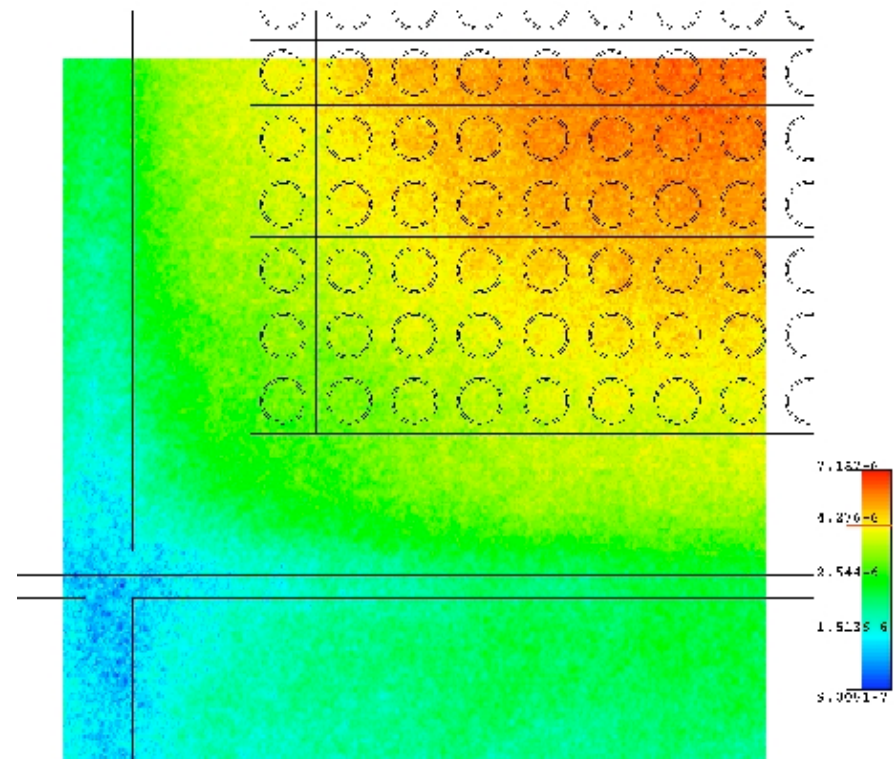
- **Using "0" as the material number on an FM card for mesh tallies causes the mesh tallies to use the true materials from the geometry**

   FM card format: FMn C m R1 R2   <—- set m=0

- **Can use this feature to edit power distributions (e.g., fission rates, energy deposition, …)**

FM134   0.069256   0   -6 -8

- **Fuel storage vault – fission distribution**
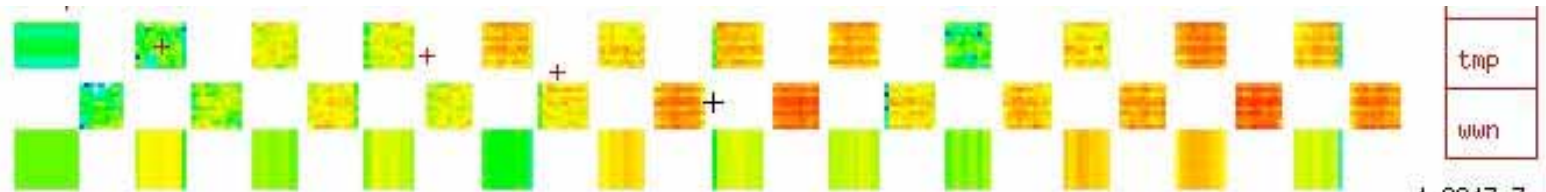
- **Detail**
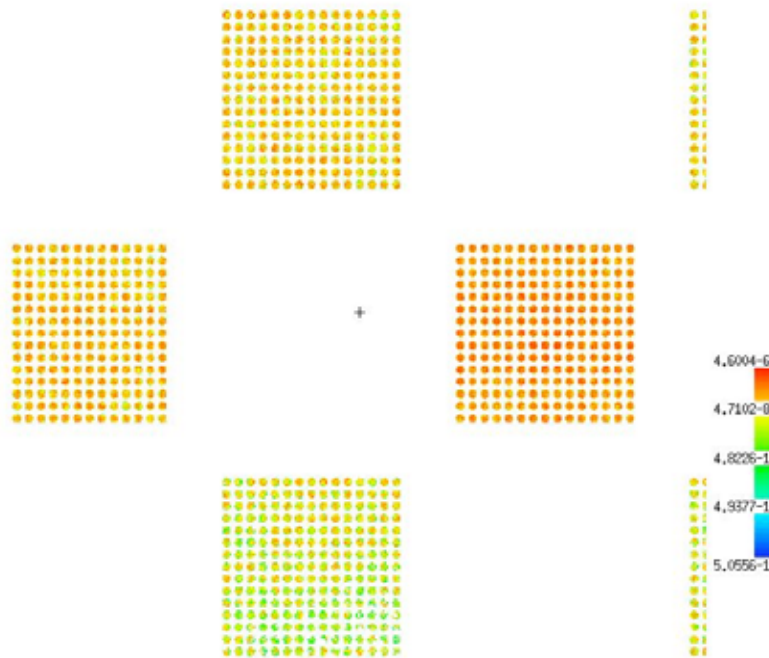
Mesh Tallies – Surface and Cell Flagging

mcnp5

Diagnostics
Applications
Group (X-5)

Los Alamos
NATIONAL LABORATORY

Use SF and CF cards as for a regular tally, except:

- **Only one tally (the flagged tally) is produced**
- **Negative cell or surface values interpreted as "anti-flag". Scores only those particles that do not cross the surface or leave the cell**

Anti-flagged cell
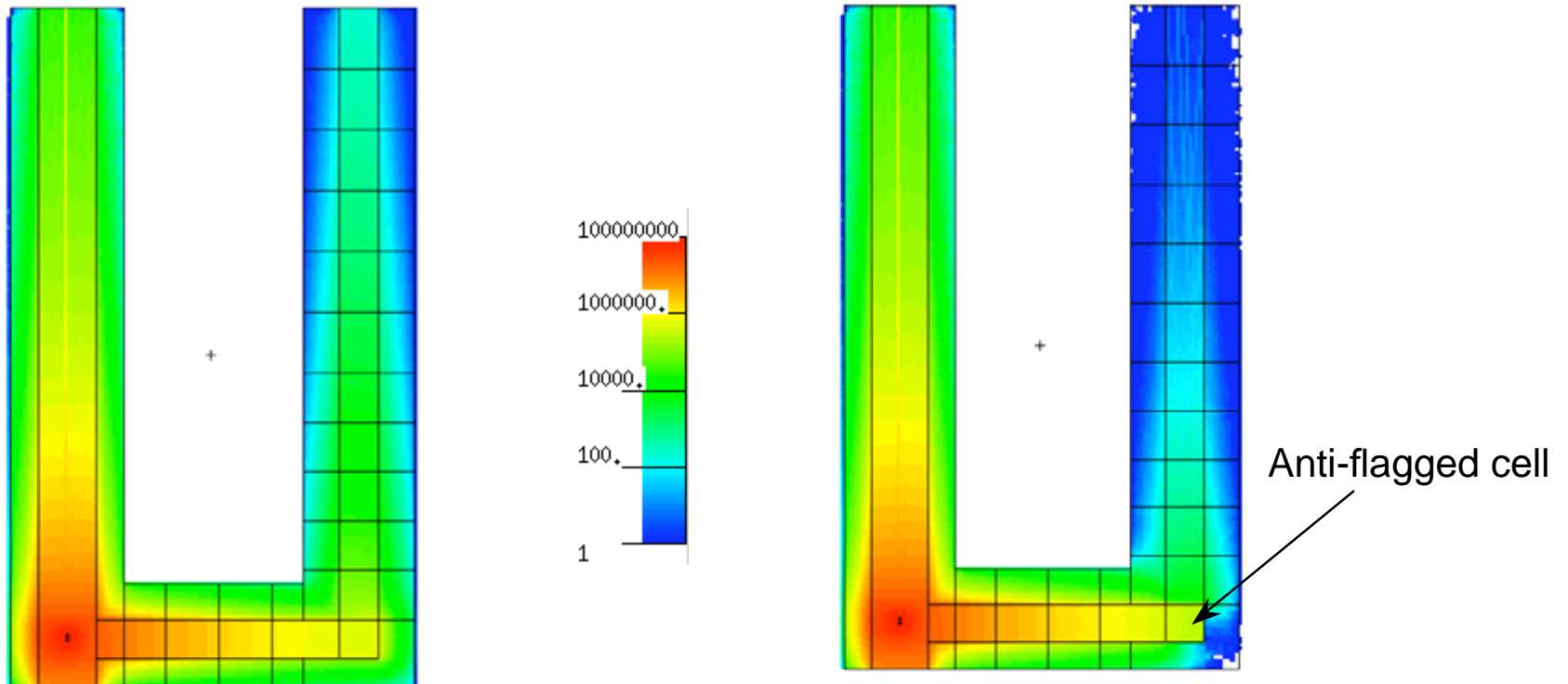
Mesh Tallies – Plotting Particle Tracks

mcnp5

Los Alamos
NATIONAL LABORATORY

By using a very fine mesh, particle tracks from individual histories can be plotted.

2000 x 1100 x 1 mesh

mcnp5

**Diagnostics
Applications
Group (X-5)**

Los Alamos
NATIONAL LABORATORY
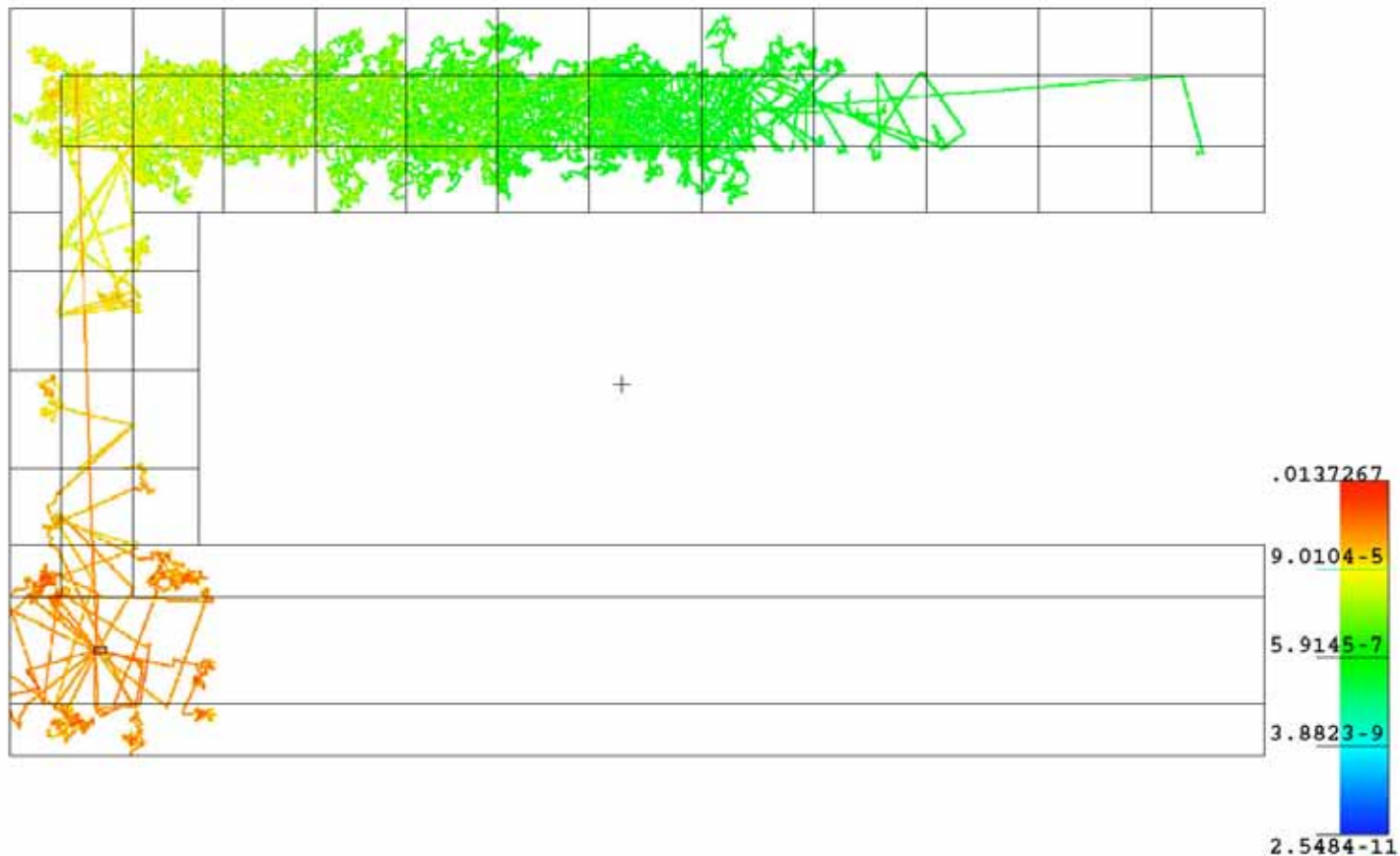
Nuclear Data for MCNP

- **Nuclear data libraries for MCNP: ENDF/B-VI and Later**

- **Temperature-specific nuclear data libraries and the DOPPLER code**

- **MCNP Criticality Validation Suite**

- **Criticality Results with ENDF/B-VI and preliminary ENDF/B-VII nuclear data libraries**

mcnp5

**Diagnostics
Applications
Group (X-5)**

Los Alamos
NATIONAL LABORATORY

NUCLEAR DATA LIBRARIES FOR MCNP:

ENDF/B-VI AND LATER

Continuous-energy Nuclear Data Libraries

mcnp5

Los Alamos

Library	Issued	Source	Identifiers	Total Nuclides	Nuclides with Probability Tables for Unresolved Resonance Region	Fissioning Nuclides with Delayed-Neutron Spectra
ENDF60	1994	ENDF/B-VI.2	.60c	122	0	0
ENDF66	2002	ENDF/B-VI.6	.64c, .65c, .66c	173	67	22
ACTI	2002	ENDF/B-VI.8	.61c, .62c, .63c	41	4	0
T16_2003	2004	LANL T-16	.67c, .69c, .68c	15	13	14

77 K   **293 K**   **3000 K**

mcnp5

- **The final release of ENDF/B-VI, ENDF/B-VI.8, was distributed in October 2001**

- ACTI can be combined with ENDF66 to produce a nuclear data library that corresponds to the final release of ENDF/B-VI for almost all nuclides

- The combination of ACTI and ENDF66 hereafter will be referred to as ENDF/B-VI

- T16_2003 was developed by LANL nuclear physics group (T-16)

- T16_2003 contains data for ^{3}H, the uranium isotopes, ^{237}Np, ^{239}Pu, ^{241}Am, and ^{243}Am

- The most notable changes in T16_2003 involve inelastic and elastic scattering cross sections, fission spectra, and the average number of neutrons emitted per fission.

- **SAB2002, a library of thermal scattering laws S(α,β), was released in 2002**

- Data in SAB2002 are derived from ENDF/B-VI (ENDF/B-VI.3)

- SAB2002 contains data for 15 combinations of nuclides and materials

- Typical temperature ranges are from 294 K to 1200 K, in increments of 200

- Data typically are tabulated at 16 angles and 64 energies for each temperature

- Data are provided at ~ 20 K for a limited number of nuclides

- **CSEWG currently plans to release the initial version of ENDF/B-VII in December 2005**

- LANL group T-16 has contributed new evaluations for ^{1}H, the uranium isotopes, ^{237}Np, and ^{239}Pu

- Principal change to data for ^{1}H is a slight reduction in its thermal capture cross section

- Changes to the data for the actinides are similar to those incorporated into T16_2003 but are more extensive

- Cross sections for ^{233}U, ^{235}U, and ^{238}U incorporate revised resonance data from Oak Ridge National Laboratory

mcnp5

**Diagnostics
Applications
Group (X-5)**

Los Alamos
NATIONAL LABORATORY

TEMPERATURE-SPECIFIC

NUCLEAR DATA LIBRARIES

AND

THE DOPPLER CODE

- **Temperature effects on Monte Carlo calculations**

  – **Dimensions for geometry**

  – **Density of materials**

  – **Cross-section data**

    • Doppler broadening of **resolved resonances** (explicit profiles)
    • Doppler broadening of **unresolved resonances** (probability tables)
    • Changes in **S(α,β) thermal scattering kernel**
    • **Elastic scattering cross-section** is Doppler broadened over entire energy range

- **For most Monte Carlo codes, temperature effects must be handled explicitly by the code users**

  – **Input changes are required to account for dimension & density changes**

  – **Must use cross-section data generated at the correct problem temperatures**

  – **MCNP automatically Doppler broadens the elastic scattering cross-sections**

  – **MCNP does NOT adjust:**

    • **resolved resonance data**
    • **unresolved resonance data**
    • **thermal scattering kernels**

- **Generation of problem-dependent cross-section datasets**
  - Use NJOY (or similar cross-section processing code) to generate nuclear cross-section datasets (called ACE datasets for MCNP)
  - Must generate a separate dataset **for each nuclide at each problem temperature**
  - NJOY routines take care of Doppler broadening (resolved & unresolved) & thermal scattering kernels
  - Can be done, but time-consuming & error-prone

- **DOPPLER code (new)**
  - Subset of NJOY routines, easy to use
  - For ACE datasets (for MCNP) performs
    - **Doppler broadening of resolved resonance data** (explicit profiles)
    - **Interpolation of unresolved resonance data (probability tables)** between ACE datasets at 2 different temperatures
    - **Interpolation of thermal scattering kernels (S(α,β) data)** between ACE datasets at 2 different temperatures
  - For now, DOPPLER is run external to MCNP
  - Plan to put the DOPPLER routines in-line with the MCNP coding

mcnp5 Diagnostics Applications Group (X-5) • Los Alamos NATIONAL LABORATORY

Kritz Benchmarks at 245 K

Case	Library	k_{eff}	Δk
Kritz:2-1	NJOY	0.9914 ± 0.0003	—
	DOPPLER	0.9911 ± 0.0003	-0.0003 ± 0.0004
Kritz:2-13	NJOY	0.9944 ± 0.0003	—
	DOPPLER	0.9942 ± 0.0003	-0.0002 ± 0.0004
Kritz:2-19	NJOY	1.0005 ± 0.0003	—
	DOPPLER	1.0009 ± 0.0003	0.0004 ± 0.0004

Conclusion: DOPPLER produces nuclear data that are consistent with those generated directly with NJOY

path=(location of initial data file)

1001.66c 0 4.386e-8 1001.01c	28061.66c 0 4.386e-8 28061.01c
5010.66c 0 4.386e-8 5010.01c	28062.66c 0 4.386e-8 28062.01c
5011.66c 0 4.386e-8 5011.01c	28064.66c 0 4.386e-8 28064.01c
8016.66c 0 4.386e-8 8016.01c	40000.66c 0 4.386e-8 40000.01c
8017.66c 0 4.386e-8 8017.01c	92235.66c 92235.65c 4.386e-8 92235.01c
24050.66c 0 4.386e-8 24050.01c	92238.66c 92238.65c 4.386e-8 92238.01c
24052.66c 0 4.386e-8 24052.01c	94239.66c 94239.65c 4.386e-8 94239.01c
24053.66c 0 4.386e-8 24053.01c	94240.66c 94240.65c 4.386e-8 94240.01c
24054.66c 0 4.386e-8 24054.01c	94241.66c 94241.65c 4.386e-8 94241.01c
26054.66c 0 4.386e-8 26054.01c	94242.66c 94242.65c 4.386e-8 94242.01c
26056.66c 0 4.386e-8 26056.01c	95241.66c 95241.65c 4.386e-8 95241.01c
26057.66c 0 4.386e-8 26057.01c	lwtr.61t lwtr.62t 4.386e-8 lwtr.01t
26058.66c 0 4.386e-8 26058.01c	end
28058.66c 0 4.386e-8 28058.01c	
28060.66c 0 4.386e-8 28060.01c	

Availability of DOPPLER

mcnp5

Diagnostics
Applications
Group (X-5)

Los Alamos
NATIONAL LABORATORY

- **DOPPLER currently is in use by LANL, LANL contractors, and other DOE laboratories**

- **It is anticipated that DOPPLER will be included, in some form, in future MCNP distributions**

- **"Pseudo-materials" for temperature dependence**
  - Also called "stochastic interpolation"
  - To approximate the cross-sections for nuclide X at temperature T, use a **weighted combination of nuclide X at lower temperature T$_1$ & higher temperature T$_2$**

$$W_2 = \frac{\sqrt{T}-\sqrt{T_1}}{\sqrt{T_2}-\sqrt{T_1}}, \qquad W_1 = 1 - W_2$$

$$\Sigma(T) = W_1 \cdot \Sigma_1 + W_2 \cdot \Sigma_2$$

  - **Example**: **^{235}U at 500 K**

    Existing datasets for MCNP:

    dataset for ^{235}U at **293.6** K: **92235.66c**

    dataset for ^{235}U at **3000.1** K: **92235.65c**

    Weight the datasets using T$^{1/2}$ interpolation

$$W_2 = \frac{\sqrt{500}-\sqrt{293.6}}{\sqrt{3000.1}-\sqrt{293.6}} = .138845, \quad W_1 = .861155$$

    In the MCNP input:

    m1   92235.66c   .861155   92235.65c   .138845

- **VHTGR model, with temperatures from the ATHENA code**
  - For pseudo-materials, explicit MCNP datasets at 100 K intervals used for temperature interpolation
  - Reference calculation used explicit MCNP datasets from NJOY at exact problem temperatures
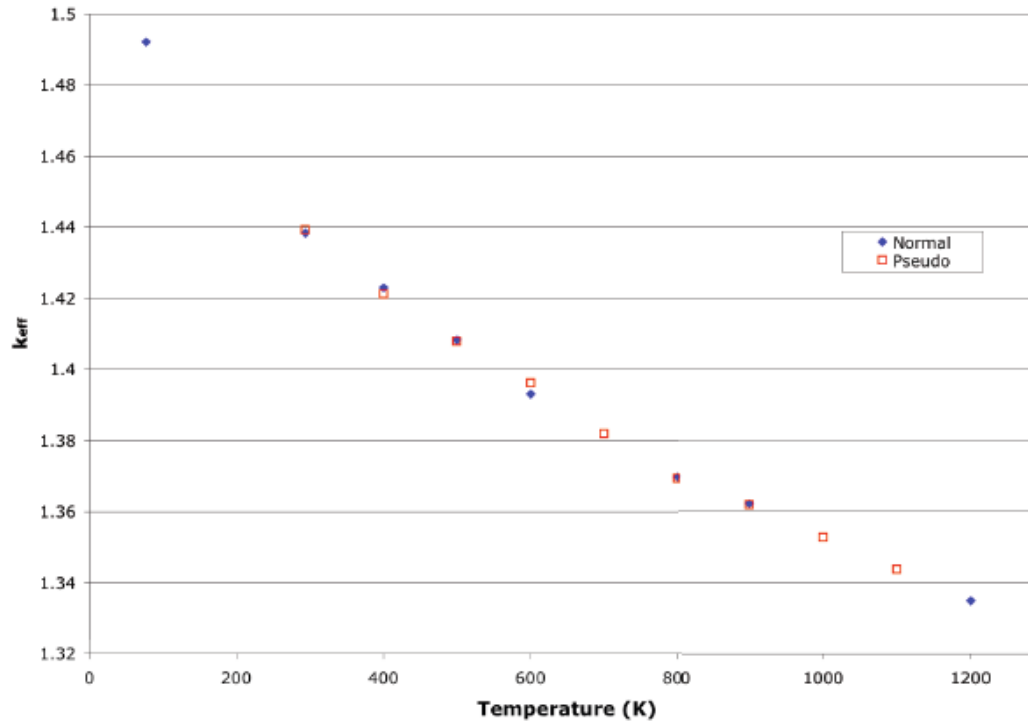
Figure 1. Comparison of k_{eff} between normal and pseudo materials with the VHTGR geometry.

JL Conlin, W Ji, JC Lee, WR Martin, "Pseudo-Material Construct for Coupled Neutronic-Thermal-Hydraulic Analysis of VHTGR", Trans. ANS 91 (2005)

- **Pseudo-material method – Advantages**

  - **Save memory storage**

    If 100s or 1000s of temperatures are needed, can "interpolate" between datasets at just 2 temperatures, rather than storing 100s or 1000s of datasets

  - **No data preprocessing required**

- **Pseudo-material method – Disadvantages**

  - **Approximate treatment**

    During the Monte Carlo calculation, picking one or the other dataset - not really interpolating

  - **Can't be used for S(α,β) thermal scattering kernels**

    Need to pick S(α,β) dataset at nearest temperature

MCNP CRITICALITY VALIDATION SUITE

- Cases were selected to encompass a wide variety of

  - Fissile isotopes : ^{233}U, ^{235}U, and ^{239}Pu
  - Spectra   :   Fast, intermediate, and thermal
  - Compositions   :   Metals, oxides, and solutions
  - Configurations   :   Bare and reflected spheres and cylinders, 2-D and 3-D lattices, and infinite homogeneous and heterogeneous regions

- ^{235}U Cases were subdivided into HEU, IEU, and LEU

- Input specifications for all 31 cases are taken from the *International Handbook of Evaluated Criticality Safety Benchmark Experiments*

Cases in the MCNP Criticality Validation Suite

| Spectrum | Fast | | | Intermed | Thermal | |
Geometry	Bare	Heavy Reflector	Light Reflector	Any	Lattice of Fuel Pins	Solution
^{233}U	Jezebel-233	Flattop-23	U233-MF-05	Falstaff-1*	SB-2½	ORNL-11
HEU	Godiva Tinkertoy-2	Flattop-25	Godiver	Zeus-2 UH$_3$	SB-5	ORNL-10
IEU	IEU-MF-03	BIG TEN	IEU-MF-04	Zebra-8H[†]	IEU-CT-02	STACY-36
LEU					B&W XI-2	LEU-ST-02
Pu	Jezebel Jezebel-240 Pu Buttons	Flattop-Pu THOR	Pu-MF-11	HISS/HPG[†]	PNL-33	PNL-2

* Extrapolated to critical
[†] k_∞ measurement

Criticality Validation Suite

Name	Spectrum	Handbook ID	Description
Jezebel-233	Fast	U233-MET-FAST-001	Bare sphere of ^{233}U
Flattop-23	Fast	U233-MET-FAST-006	Sphere of ^{233}U reflected by normal U
U233-MF-05	Fast	U233-MET-FAST-005, case 2	Sphere of ^{233}U reflected by beryllium
Falstaff-1	Intermediate	U233-SOL-INTER-001, case 1	Sphere of uranyl fluoride solution enriched in ^{233}U
SB-2½	Thermal	U233-COMP-THERM-001, case 3	Lattice of ^{233}U fuel pins in water
ORNL-11	Thermal	U233-SOL-THERM-008	Large sphere of uranyl nitrate solution enriched in ^{233}U
Godiva	Fast	HEU-MET-FAST-001	Bare HEU sphere
Tinkertoy-2	Fast	HEU-MET-FAST-026, case C-11	3 x 3 x 3 array of HEU cylinders in paraffin box
Flattop-25	Fast	HEU-MET-FAST-028	HEU sphere reflected by normal U
Godiver	Fast	HEU-MET-FAST-004	HEU sphere reflected by water
Zeus-2	Intermediate	HEU-MET-INTER-006, case 2	HEU platters moderated by graphite and reflected by copper
UH$_3$	Intermediate	HEU-COMP-INTER-003, case 6	UH$_3$ cylinders reflected by depleted uranium
SB-5	Thermal	U233-COMP-THERM-001, case 6	Lattice of HEU fuel pins in water, with blanket of ThO$_2$ pins
ORNL-10	Thermal	HEU-SOL-THERM-032	Large sphere of HEU nitrate solution
IEU-MF-03	Fast	IEU-MET-FAST-003	Bare sphere of IEU (36 wt.%)
BIG TEN	Fast	IEU-MET-FAST-007	Cylinder of IEU (10 wt.%) reflected by normal uranium
IEU-MF-04	Fast	IEU-MET-FAST-004	Sphere of IEU (36 wt.%) reflected by graphite
Zebra-8H	Intermediate	MIX-MET-FAST-008, case 7	IEU (37.5 wt.%) reflected by normal U and steel
IEU-CT-02	Thermal	IEU-COMP-THERM-002, case 3	Lattice of IEU (17 wt.%) fuel rods in water
STACY-36	Thermal	LEU-SOL-THERM-007, case 36	Cylinder of IEU (9.97 wt.%) uranyl nitrate solution
B&W XI-2	Thermal	LEU-COMP-THERM-008, case 2	Large lattice of LEU (2.46 wt.%) fuel pins in borated water
LEU-ST-02	Thermal	LEU-SOL-THERM-002, case 2	Sphere of LEU (4.9 wt.%) uranyl fluoride solution
Jezebel	Fast	PU-MET-FAST-001	Bare sphere of plutonium
Jezebel-240	Fast	PU-MET-FAST-002	Bare sphere of plutonium (20.1 at.% ^{240}Pu)
Pu Buttons	Fast	PU-MET-FAST-003, case 103	3 x 3 x 3 array of small cylinders of plutonium
Flattop-Pu	Fast	PU-MET-FAST-006	Plutonium sphere reflected by normal U
THOR	Fast	PU-MET-FAST-006	Plutonium sphere reflected by thorium
PU-MF-11	Fast	PU-MET-FAST-011	Plutonium sphere reflected by water
HISS/HPG	Intermediate	PU-COMP-INTER-001	Infinite, homog. mixture of plutonium, hydrogen, & graphite
PNL-33	Thermal	MIX-COMP-THERM-002, case 4	Lattice of mixed-oxide fuel pins in borated water
PNL-2	Thermal	PU-SOL-THERM-021, case 3	Sphere of plutonium nitrate solution

Diagnostics Applications Group (X-5)

mcnp5

Los Alamos

Purpose & Use of the MCNP Criticality Validation Suite

- The MCNP Criticality Validation Suite was developed to assess the reactivity impact of future improvements to MCNP as well as changes to its associated nuclear data libraries

- Suite is *not* an absolute indicator of the accuracy or reliability of a given nuclear data library, nor is it intended to be

- Suite can provide a general indication of the overall performance of a nuclear data library

- Suite can provide an early warning of unexpected or unintended consequences resulting from changes to nuclear data

CRITICALITY RESULTS WITH

ENDF/B-VI AND PRELIMINARY ENDF/B-VII

NUCLEAR DATA LIBRARIES

MCNP5 Calculations for Criticality Val. Suite

mcnp5

**Diagnostics
Applications
Group (X-5)**

Los Alamos
NATIONAL LABORATORY

- Each calculation employed 550 generations with 10,000 neutrons per generation (SB-5 and Zebra-8H employed 350 generations)

- Results from first 50 generations were excluded from the statistics

- Results therefore are based on 5,000,000 active histories for each case (3,000,000 for SB-5 and Zebra-8H)

- All calculations with thermal scattering laws used SAB2002

- ENDF/B-VI data were used for nuclides not present in T16_2003 and initial ENDF/B-VII libraries when those calculations were performed

Case	Benchmark k_{eff}	Calculated k_{eff}			
		ENDF/B-VII	T16_2003	ENDF/B-VI	ENDF60
Jezebel-233	1.0000±0.0010	0.9997±0.0003	0.9989±0.0002	0.9926±0.0002	0.9928±0.0003
Flattop-23	1.0000±0.0014	0.9994±0.0003	0.9985±0.0003	1.0003±0.0003	1.0008±0.0003
U233-MF-05	1.0000±0.0030	0.9979±0.0003	0.9972±0.0005	0.9972±0.0003	0.9971±0.0003
Falstaff-1	1.0000±0.0083	0.9906±0.0005	0.9873±0.0005	0.9895±0.0005	0.9890±0.0005
SB-2½	1.0000±0.0024	0.9988±0.0004	0.9951±0.0005	0.9964±0.0005	0.9978±0.0005
ORNL-11	1.0006±0.0029	1.0041±0.0002	1.0006±0.0002	0.9974±0.0002	0.9956±0.0002

$1\sigma < \Delta k \leq 2\sigma$ $\Delta k > 2\sigma$

- ENDF/B-VII and T16_2003 produce significant improvements relative to ENDF/B-VI and ENDF60

- ENDF/B-VII and T16_2003 eliminate reactivity swings between Jezebel-233 and Flattop-23

Case	Benchmark k_{eff}	Calculated k_{eff}			
		ENDF/B-VII	T16_2003	ENDF/B-VI	ENDF60
Godiva	1.0000±0.0010	0.9994±0.0003	0.9990±0.0003	0.9963±0.0003	0.9965±0.0003
Tinkertoy-2	1.0000±0.0038	1.0004±0.0003	1.0001±0.0003	0.9973±0.0003	0.9987±0.0003
Flattop-25	1.0000±0.0030	1.0029±0.0003	1.0023±0.0005	1.0021±0.0003	1.0027±0.0003
Godiver	0.9985±0.0011	0.9978±0.0003	0.9969±0.0004	0.9948±0.0003	0.9970±0.0003
UH_3	1.0000±0.0047	0.9952±0.0003	0.9925±0.0003	0.9914±0.0003	1.0080±0.0004
Zeus-2	0.9997±0.0008	0.9958±0.0004	0.9951±0.0003	0.9942±0.0003	1.0088±0.0004
SB-5	1.0015±0.0028	0.9957±0.0005	0.9941±0.0005	0.9965±0.0005	0.9972±0.0005
ORNL-10	1.0015±0.0026	0.9989±0.0002	0.9986±0.0002	0.9992±0.0002	0.9970±0.0002

- ENDF/B-VII and T16_2003 produce significant improvements for fast cases

- ENDF/B-VII produces additional improvements for Godiver, epithermal cases, and ORNL-10 (probably due to improved representation for low-lying resonances)

Case	Benchmark k_{eff}	Calculated k_{eff}			
		ENDF/B-VII	T16_2003	ENDF/B-VI	ENDF60
IEU-MF-03	1.0000±0.0017	1.0027±0.0003	1.0029±0.0003	0.9987±0.0003	1.0001±0.0003
BIG TEN	0.9948±0.0013	0.9952±0.0003	0.9952±0.0003	1.0071±0.0003	1.0043±0.0002
IEU-MF-04	1.0000±0.0030	1.0072±0.0003	1.0080±0.0003	1.0036±0.0003	1.0044±0.0003
Zebra-8H	1.0300±0.0025	1.0198±0.0002	1.0197±0.0002	1.0406±0.0002	1.0304±0.0002
IEU-CT-02	1.0017±0.0044	1.0008±0.0003	0.9998±0.0003	1.0004±0.0003	1.0010±0.0003
STACY-36	0.9988±0.0013	0.9994±0.0003	0.9973±0.0003	0.9986±0.0003	0.9964±0.0003

ENDF/B-VII and T16_2003 produce much better results for BIG TEN but worse results for other fast cases

Results for LEU Benchmarks

mcnp5

Diagnostics
Applications
Group (X-5)

Los Alamos
NATIONAL LABORATORY

Case	Benchmark k_{eff}	Calculated k_{eff}			
		ENDF/B-VII	T16_2003	ENDF/B-VI	ENDF60
B&W XI-2	1.0007±0.0012	1.0000±0.0003	0.9978±0.0003	0.9968±0.0003	0.9965±0.0003
LEU-ST-02	1.0024±0.0037	0.9961±0.0003	0.9944±0.0003	0.9953±0.0003	0.9916±0.0003

- ENDF/B-VII produces significant improvement for B&W XI-2 (eliminates long-standing problem with capture in low-lying ^{238}U resonances)

- Combination of slightly lower ^{1}H thermal capture cross section and improved resonance data in ENDF/B-VII produce improved result for LEU-ST-02

Results for Pu Benchmarks

Case	Benchmark k_{eff}	Calculated k_{eff}			
		ENDF/B-VII	T16_2003	ENDF/B-VI	ENDF60
Jezebel	1.0000±0.0020	0.9998±0.0003	1.0003±0.0003	0.9971±0.0003	0.9974±0.0003
Jezebel-240	1.0000±0.0020	1.0003±0.0003	1.0000±0.0003	0.9980±0.0003	0.9985±0.0003
Pu Buttons	1.0000±0.0030	0.9984±0.0003	0.9994±0.0003	0.9962±0.0003	0.9969±0.0003
Flattop-Pu	1.0000±0.0030	1.0004±0.0003	1.0008±0.0004	1.0016±0.0003	1.0032±0.0003
THOR	1.0000±0.0006	1.0079±0.0003	1.0079±0.0003	1.0057±0.0003	1.0062±0.0003
Pu-MF-11	1.0000±0.0010	0.9992±0.0004	0.9987±0.0003	0.9966±0.0003	0.9980±0.0004
HISS/HPG	1.0000±0.0110	1.0106±0.0002	1.0104±0.0002	1.0106±0.0003	1.0105±0.0002
PNL-33	1.0024±0.0021	1.0063±0.0003	1.0051±0.0003	1.0029±0.0003	1.0015±0.0003
PNL-2	1.0000±0.0065	1.0029±0.0005	1.0036±0.0005	1.0031±0.0005	1.0006±0.0005

- ENDF/B-VII and T16_2003 produce improved results for fast cases except THOR

- JEFF 3.1 cross sections for ^{232}Th reduce k_{eff} for THOR to 1.0025 ± 0.0003

SUMMARY OF RESULTS FOR
MCNP CRITICALITY VALIDATION SUITE

Range	ENDF/B-VII	T16_2003	ENDF/B-VI	ENDF60
$|\Delta k| \leq \sigma$	21	15	13	12
$\sigma < |\Delta k| \leq 2\sigma$	5	9	9	10
$|\Delta k| > 2\sigma$	5	7	9	9

- ENDF/B-VII produces best overall results, by far

Data testing with MCNP5 has identified several areas of concern for ENDF/B-VII:

- **Unresolved resonance region for ^{235}U**

- **Fast cross sections for ^{232}Th**

- **Fast cross sections for ^{237}Np**

- **Fast cross sections for Cu**

- **Thermal cross sections for ^{233}U and ^{239}Pu**

- **Angular scattering distribution for ^{2}H**

mcnp5

**Diagnostics
Applications
Group (X-5)**

Los Alamos
NATIONAL LABORATORY

Monte Carlo Criticality Calculations

-

Power Iteration, Convergence,

& Weilandt's Method

K-eigenvalue equation

Diagnostics
Applications
Group (X-5)

mcnp5

Los Alamos
NATIONAL LABORATORY

$$\left[\vec{\Omega} \cdot \nabla + \Sigma_T(\vec{r},E) \right] \Psi_k(\vec{r},E,\vec{\Omega}) = \iint \Psi_k(\vec{r},E',\vec{\Omega}')\Sigma_S(\vec{r},E' \to E,\vec{\Omega} \cdot \vec{\Omega}')d\vec{\Omega}'dE'$$

$$+ \frac{1}{K_{eff}} \cdot \frac{\chi(E)}{4\pi} \iint \nu\Sigma_F(\vec{r},E')\Psi_k(\vec{r},E',\vec{\Omega}')d\vec{\Omega}'dE'$$

where

K_{eff} = k-effective, eigenvalue for fundamental mode

$\Psi_k(\vec{r},E,\vec{\Omega})$ = angular flux, for fundamental k-eigenmode

$\vec{\Omega} \cdot \nabla \Psi_k(\vec{r},E,\vec{\Omega})$ = loss term, leakage

$\Sigma_T(\vec{r},E) \Psi_k(\vec{r},E,\vec{\Omega})$ = loss term, collisions

$\iint \Psi_k(\vec{r},E',\vec{\Omega}')\Sigma_S(\vec{r},E' \to E,\vec{\Omega} \cdot \vec{\Omega}')d\vec{\Omega}'dE'$ = gain term, scatter from E',Ω' into E,Ω

$\frac{1}{K_{eff}} \cdot \frac{\chi(E)}{4\pi} \iint \nu\Sigma_F(\vec{r},E')\Psi_k(\vec{r},E',\vec{\Omega}')d\vec{\Omega}'dE'$ = gain term, production from fission

$\Rightarrow$ **Jointly find K_{eff} and $\Psi_k(r,E,\Omega)$ such that equation balances**

K-eigenvalue equation

- Use operator (or matrix) form to simplify notation

$$(L + T)\Psi = S\Psi + \frac{1}{K_{eff}}M\Psi$$

where

$$L = \text{leakage operator} \qquad S = \text{scatter-in operator}$$
$$T = \text{collision operator} \qquad M = \text{fission multiplication operator}$$

- Rearrange

$$(L + T - S)\Psi = \frac{1}{K_{eff}}M\Psi$$

$$\Psi = \frac{1}{K_{eff}} \cdot (L + T - S)^{-1}M\Psi$$

$$\Psi = \frac{1}{K_{eff}} \cdot F\Psi$$

$\Rightarrow$ **This eigenvalue equation will be solved by <u>power iteration</u>**

Eigenvalue equation

$$\Psi = \frac{1}{K_{eff}} \cdot F\Psi$$

1. **Assume that k_{eff} and Ψ on the right side are known for iteration n, solve for Ψ on left side (for iteration n+1)**

$$\Psi^{(n+1)} = \frac{1}{K_{eff}^{(n)}} \cdot F\Psi^{(n)}$$

Note: This requires solving the equation below for $\Psi^{(n+1)}$, with $K_{eff}^{(n)}$ and $\Psi^{(n)}$ fixed

$$(L + T - S)\Psi^{(n+1)} = \frac{1}{K_{eff}^{(n)}} M\Psi^{(n)}$$

2. **Then, compute $K_{eff}^{(n+1)}$**

$$K_{eff}^{(n+1)} = K_{eff}^{(n)} \cdot \frac{\int M\Psi^{(n+1)} d\vec{r}}{\int M\Psi^{(n)} d\vec{r}}$$ (other norms could be used)
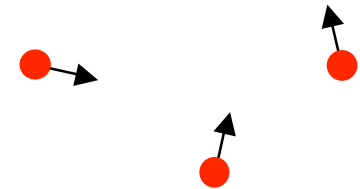
- **Power iteration procedure:**

    1. **Initial guess for K_{eff} and Ψ**

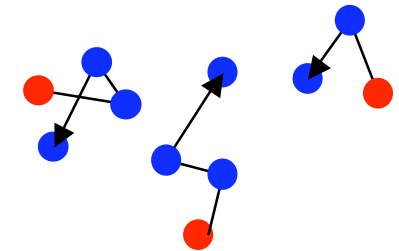 $K_{eff}^{(0)}, \quad \Psi^{(0)}$

       Source points for $\Psi^{(0)}$

    2. **Solve for $\Psi^{(n+1)}$ [Monte Carlo random walk for N particles]**

       $$\Psi^{(n+1)} = \frac{1}{K_{eff}^{(n)}} \cdot F\Psi^{(n)}$$
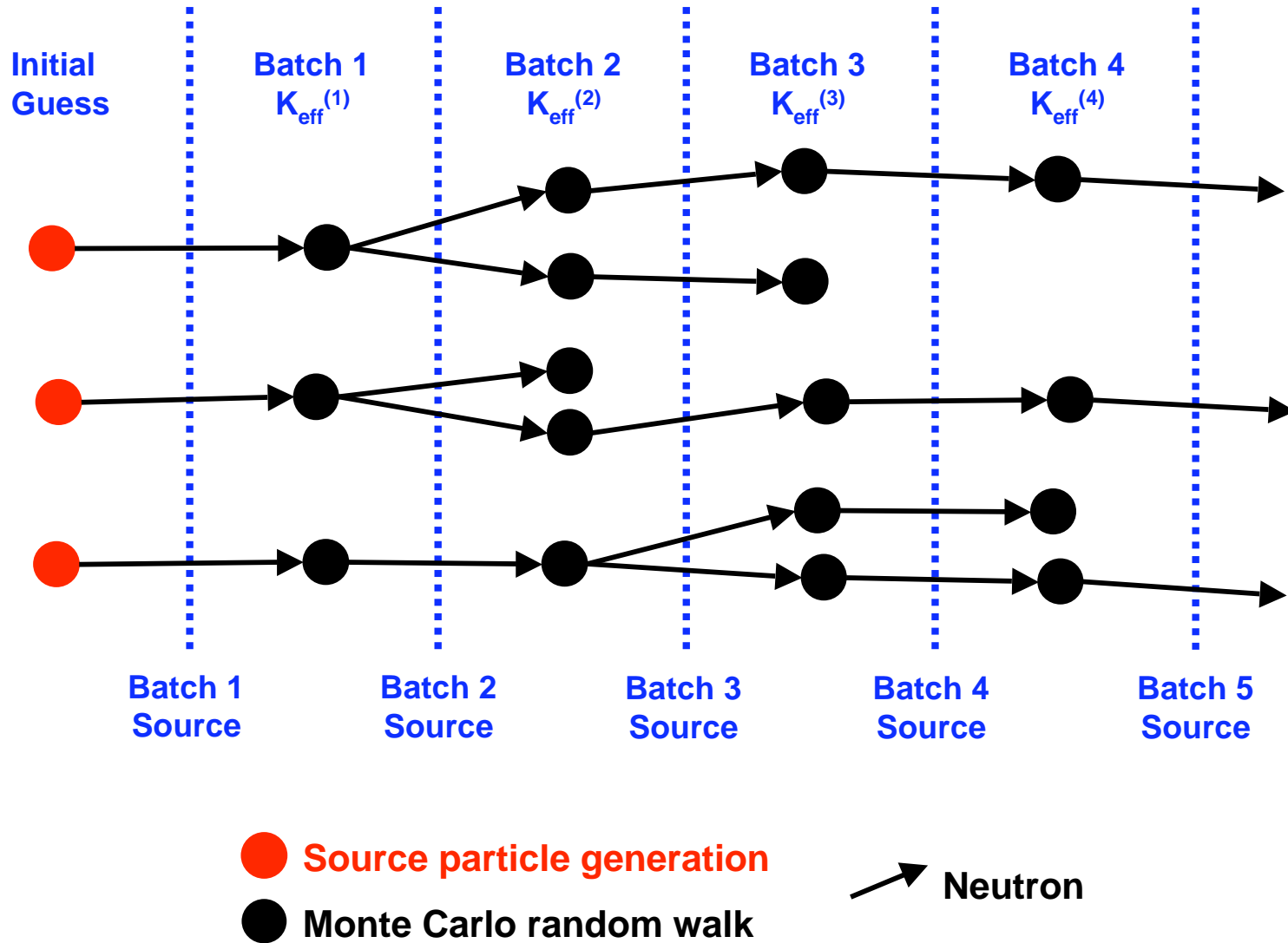
       Source points for $\Psi^{(n+1)}$

    3. **Compute new K_{eff}**

       $$K_{eff}^{(n+1)} = K_{eff}^{(n)} \cdot \frac{\int M\Psi^{(n+1)} d\vec{r}}{\int M\Psi^{(n)} d\vec{r}}$$

    4. **Repeat 1–3 until both $K_{eff}^{(n+1)}$ and $\Psi^{(n+1)}$ have converged**

Power Iteration

- **Power iteration for Monte Carlo k-effective calculation**

Initial Guess

Batch 1 $K_{eff}^{(1)}$

Batch 2 $K_{eff}^{(2)}$

Batch 3 $K_{eff}^{(3)}$

Batch 4 $K_{eff}^{(4)}$

Batch 1 Source

Batch 2 Source

Batch 3 Source

Batch 4 Source

Batch 5 Source

● Source particle generation

● Monte Carlo random walk

↗ Neutron

mcnp5

**Diagnostics
Applications
Group (X-5)**

Los Alamos
NATIONAL LABORATORY

Diffusion Theory or Discrete-ordinates Transport

1. Initial guess for K_{eff} and Ψ

$$K_{eff}^{(0)}, \quad \Psi^{(0)}$$

2. Solve for $\Psi^{(n+1)}$

Inner iterations over space or space/angle to solve for $\Psi^{(n+1)}$

$$(L + T - S)\Psi^{(n+1)} = \frac{1}{K_{eff}^{(n)}} M\Psi^{(n)}$$

3. Compute new K_{eff}

$$K_{eff}^{(n+1)} = K_{eff}^{(n)} \cdot \frac{1iM\Psi^{(n+1)}}{1iM\Psi^{(n)}}$$

4. Repeat 1–3 until both $K_{eff}^{(n+1)}$ and $\Psi^{(n+1)}$ have converged

Monte Carlo

1. Initial guess for K_{eff} and Ψ

$$K_{eff}^{(0)}, \quad \Psi^{(0)}$$

2. Solve for $\Psi^{(n+1)}$

Follow particle histories to solve for $\Psi^{(n+1)}$

$$(L + T - S)\Psi^{(n+1)} = \frac{1}{K_{eff}^{(n)}} M\Psi^{(n)}$$

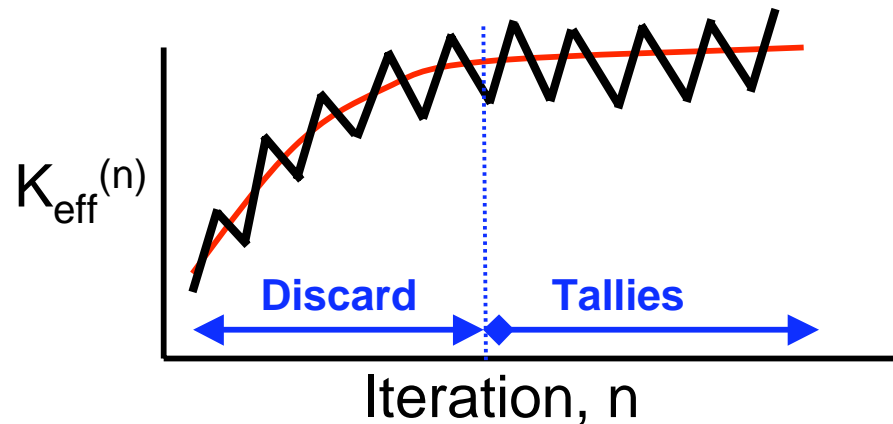**During histories, save fission sites to use for source in next iteration**

3. Compute new K_{eff}

During histories for iteration (n+1), estimate $K_{eff}^{(n+1)}$

$$K_{eff}^{(n+1)} = K_{eff}^{(n)} \cdot \frac{\int M\Psi^{(n+1)} d\vec{r}}{\int M\Psi^{(n)} d\vec{r}}$$

4. Repeat 1–3 until both $K_{eff}^{(n+1)}$ and $\Psi^{(n+1)}$ have converged

5. Continue iterating, to compute tallies

Power Iteration

$K_{eff}^{(n)}$ — **Monte Carlo**

Deterministic (S_n)

Discard — **Tallies**

Iteration, n

- **Guess an initial source distribution**
- **Iterate until converged   (How do you know ???)**
- **Then**
  - **For S_n code: done, print the results**
  - **For Monte Carlo: start tallies,**
    keep running until uncertainties small enough

- **Convergence? Stationarity? Bias? Statistics?**

- **Expand Ψ in terms of eigenfunctions $u_j(r,E,\Omega)$**

$$\Psi = \sum_{j=0}^{\infty} a_j\vec{u}_j = a_0\vec{u}_0 + a_1\vec{u}_1 + a_2\vec{u}_2 + a_3\vec{u}_3 + ...$$

$$\int \vec{u}_j\vec{u}_k dV = \delta_{jk}$$

$$a_j = \int \Psi \cdot \vec{u}_j dV$$

$$\vec{u}_j = \frac{1}{k_j}F \cdot \vec{u}_j \qquad k_0 > k_1 > k_2 > ...$$

$$k_0 \equiv k_{effective}$$

Power Iteration – Convergence

mcnp5

**Diagnostics
Applications
Group (X-5)**

Los Alamos
NATIONAL LABORATORY

- **Expand the initial guess in terms of the eigenmodes**

$$\Psi^{(0)} = \sum_{j=0} a_j^{(0)} \vec{u}_j$$

- **Substitute the expansion for Ψ into eigenvalue equation**

$$\Psi^{(n+1)} = \frac{1}{K^{(n)}} F \cdot \Psi^{(n)} = \frac{1}{k^{(n)}} \cdot \frac{1}{k^{(n-1)}} \cdots \frac{1}{k^{(0)}} \cdot F^n \cdot \Psi^{(0)}$$

$$= \left[\prod_{m=0}^{n} \frac{k_0}{K^{(m)}} \right] \cdot a_0^{(0)} \cdot \left[\vec{u}_0 + \sum_{j=1} \left(\frac{a_j^{(0)}}{a_0^{(0)}} \right) \cdot \left(\frac{k_j}{k_0} \right)^{n+1} \cdot \vec{u}_j \right]$$

$$\approx \left[\text{constant} \right] \cdot \left[\vec{u}_0 + \left(\frac{a_1^{(0)}}{a_0^{(0)}} \right) \cdot \left(\frac{k_1}{k_0} \right)^{n+1} \cdot \vec{u}_1 + \left(\frac{a_2^{(0)}}{a_0^{(0)}} \right) \cdot \left(\frac{k_2}{k_0} \right)^{n+1} \cdot \vec{u}_2 + \ldots \right]$$

$$\Psi^{(n+1)} \approx [\text{constant}] \cdot \left[\vec{u}_0 + \left(\frac{a_1^{(0)}}{a_0^{(0)}} \right) \cdot \left(\frac{k_1}{k_0} \right)^{n+1} \cdot \vec{u}_1 + \left(\frac{a_2^{(0)}}{a_0^{(0)}} \right) \cdot \left(\frac{k_2}{k_0} \right)^{n+1} \cdot \vec{u}_2 + ... \right]$$

$$K^{(n+1)} \approx k_0 \cdot \frac{\left[1 + \left(\frac{a_1^{(0)}}{a_0^{(0)}} \right) \cdot \left(\frac{k_1}{k_0} \right)^{n+1} \cdot G_1 + \left(\frac{a_2^{(0)}}{a_0^{(0)}} \right) \cdot \left(\frac{k_2}{k_0} \right)^{n+1} \cdot G_2 + ... \right]}{\left[1 + \left(\frac{a_1^{(0)}}{a_0^{(0)}} \right) \cdot \left(\frac{k_1}{k_0} \right)^{n} \cdot G_1 + \left(\frac{a_2^{(0)}}{a_0^{(0)}} \right) \cdot \left(\frac{k_2}{k_0} \right)^{n} \cdot G_2 + ... \right]}$$

where $\qquad G_m = \dfrac{\int M \vec{u}_m d\vec{r}}{\int M \vec{u}_0 d\vec{r}}$

$\Rightarrow$ **Because** $\mathbf{k_0 > k_1 > k_2 > ...,}$ **all of the red terms vanish as n$\rightarrow\infty$,**

thus $\qquad \Psi^{(n+1)} \rightarrow$ **constant $\cdot$ u$_0$**

$\qquad\qquad\quad K^{(n+1)} \rightarrow k_0$

Power Iteration – Convergence

- **After n iterations, the J-th mode error component is reduced by the factor $(k_J / k_0)^n$**

- **Since $1 > k_1/k_0 > k_2/k_0 > k_3/k_0 > \ldots$,
  after the initial transient, error in $\Psi^{(n)}$ is dominated by first mode:**
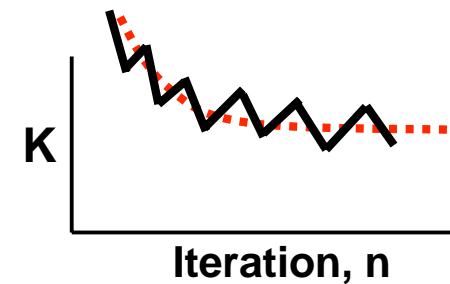
$$\Psi^{(n)} \approx [\text{cons}\tan t] \; i \left[\vec{u}_0 + \left(\frac{a_1^{(0)}}{a_0^{(0)}} \right) \cdot \left(\frac{k_1}{k_0} \right)^n \cdot \vec{u}_1 + \ldots \right]$$

- **(k_1 / k_0) is called the <u>dominance ratio</u>, DR or ρ**

  - **Errors die off as $\sim (DR)^n$**

  - To reduce 10% error $\rightarrow$ .1% error

    DR~.9 $\rightarrow$ 44 iterations
    DR~.99 $\rightarrow$ 458 iterations
    DR~.999 $\rightarrow$ 2301 iterations

Initial guess
Exact solution

Power Iteration – Convergence

mcnp5

**Diagnostics
Applications
Group (X-5)**

Los Alamos
NATIONAL LABORATORY
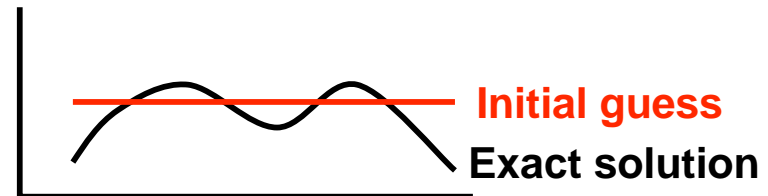
Typical K-effective convergence patterns

- **Higher mode error terms die out as $(k_J / k_0)^n$,   for n iterations**

- **When initial guess is concentrated in center of reactor, initial K_{eff} is too high** (underestimates leakage)

K

Iteration, n

- **When initial guess is uniformly distributed, initial K_{eff} is too low** (overestimates leakage)

K

Iteration, n

- The **Sandwich Method** uses 2 K_{eff} calculations - one starting too high & one starting too low. Both calculations should converge to the same result.

$$\Psi^{(n+1)} \approx [\text{constant}] \cdot \left[\vec{u}_0 + \left(\frac{a_1^{(0)}}{a_0^{(0)}} \right) \cdot \left(\frac{k_1}{k_0} \right)^{n+1} \cdot \vec{u}_1 + \ldots \right]$$

$$K^{(n+1)} \approx k_0 \cdot \frac{\left[1 + \left(\frac{a_1^{(0)}}{a_0^{(0)}} \right) \cdot \left(\frac{k_1}{k_0} \right)^{n+1} \cdot G_1 + \ldots \right]}{\left[1 + \left(\frac{a_1^{(0)}}{a_0^{(0)}} \right) \cdot \left(\frac{k_1}{k_0} \right)^{n} \cdot G_1 + \ldots \right]} \approx k_0 \cdot \left[1 + \left(\frac{a_1^{(0)}}{a_0^{(0)}} \right) \cdot \left(\frac{k_1}{k_0} \right)^{n+1} \cdot G_1 \right] \cdot \left[1 - \left(\frac{a_1^{(0)}}{a_0^{(0)}} \right) \cdot \left(\frac{k_1}{k_0} \right)^{n} \cdot G_1 \right]$$

$$\approx k_0 \cdot \left[1 + \left(\frac{a_1^{(0)}}{a_0^{(0)}} \right) \cdot \left(\frac{k_1}{k_0} \right)^{n} \cdot \left(\frac{k_1}{k_0} - 1 \right) \cdot G_1 + \ldots \right]$$

- **For problems with a high dominance ratio (e.g., DR ~ .99), the error in K_{eff} may be small, since the factor $(k_1/k_0 - 1)$ is small.**

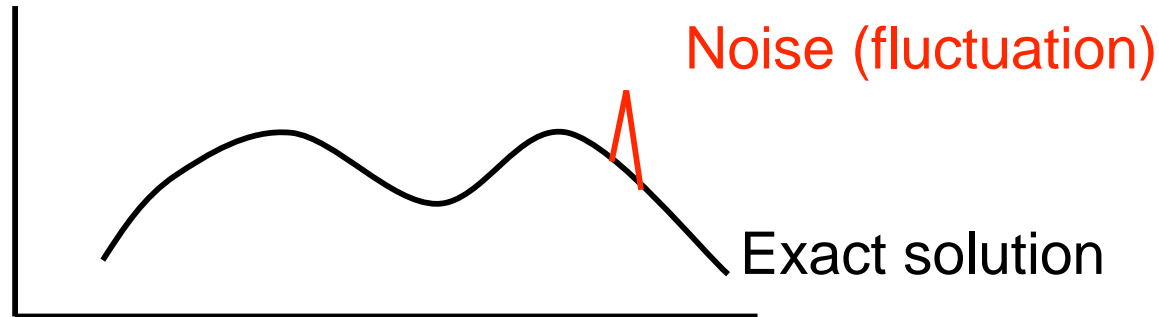⇒ **K_{eff} may appear converged, even if the source distribution is <u>not</u> converged**

- **Keff is an integral quantity – converges faster than source shape**

Keff calculation for 2 nearly symmetric slabs, with Dominance Ratio = .9925

Power Iteration – Convergence

mcnp5

Diagnostics
Applications
Group (X-5)

Los Alamos
NATIONAL LABORATORY

Noise (fluctuation)

Exact solution
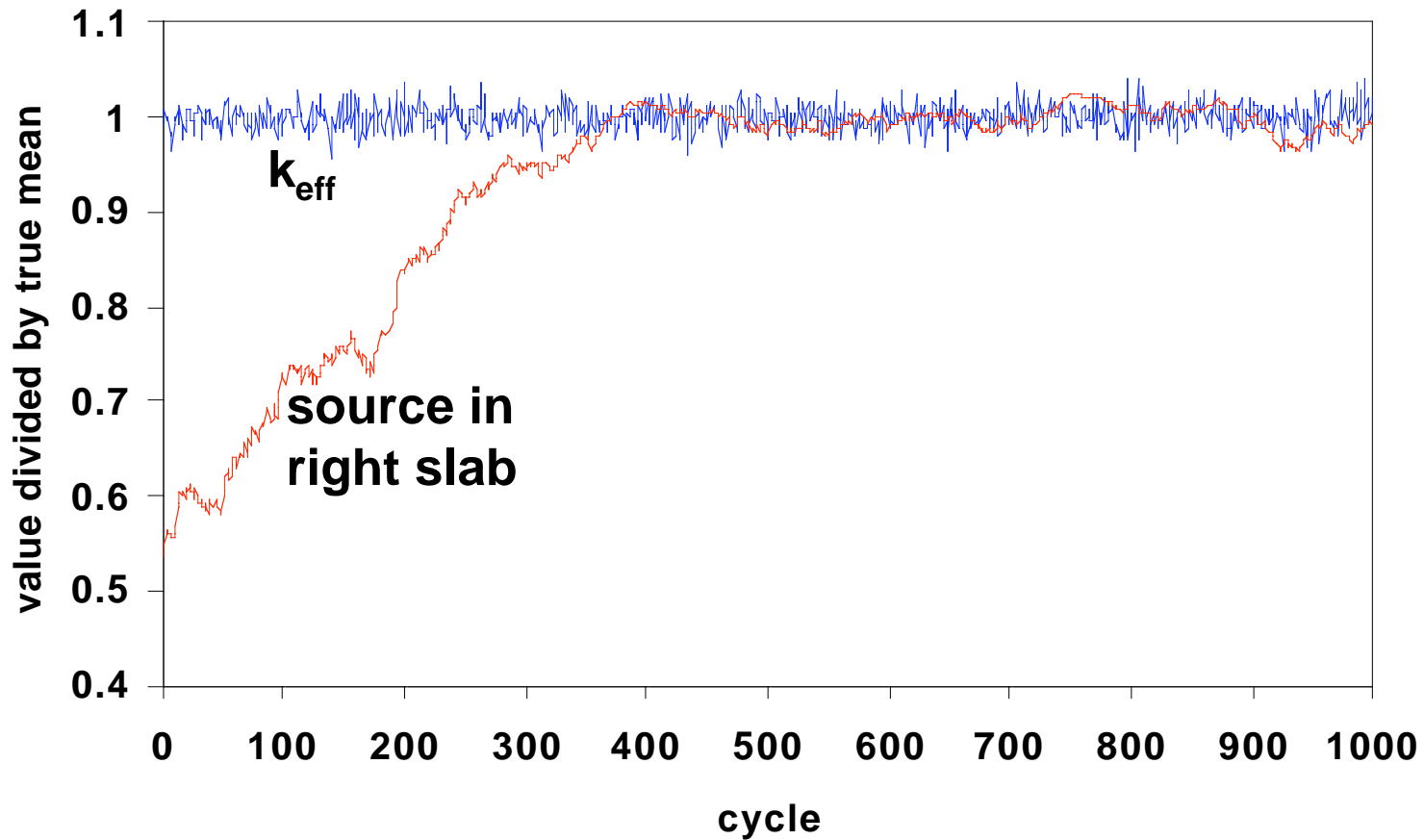
- For Monte Carlo power iteration,
  statistical fluctuations in source shape die out gradually over a
  number of successive iterations.

  – **Persistence of the noise over successive iterations gives
    correlation among source distributions in successive iterations.
    (Positive correlation)**

  – **Correlation directly affects confidence intervals:**
    **Serial correlation in the source distribution ➔ larger confidence
    intervals**

⇒ **Most Monte Carlo codes ignore these correlation effects
    & incorrectly underestimate the confidence intervals**

Summary

- **Local errors in the source distribution** decay as $(k_J/k_0)^n$

  – **Higher eigenmodes die out rapidly, convergence dominated by k_1/k_0**

  – **High DR $\rightarrow$ slow convergence**

  – **High DR $\rightarrow$ large correlation $\rightarrow$ large error in computed variances**

- **Errors in K_{eff} decay as** $(k_J/k_0 - 1) * (k_J/k_0)^n$

  – **High DR $\rightarrow$ $k_J/k_0 \sim 1$ $\rightarrow$ small error**

- **K_{eff} errors die out faster than local source errors**

  – **K_{eff} is an integral quantity – positive & negative fluctuations cancel**

- **High DR is common for**

  – Large reactors, with small leakage

  – Heavy-water moderated or reflected reactors

  – Loosely-coupled systems

$\Rightarrow$ **If local tallies are important (e.g., assembly power, pin power, …), examine their convergence – not just K_{eff} convergence**

Wielandt Method

mcnp5

Diagnostics
Applications
Group (X-5)

Los Alamos

- **Basic transport equation for eigenvalue problems**

$$(L + T - S)\Psi = \frac{1}{K_{eff}}M\Psi$$

  L = loss to leakage   S = gain from scatter-in

  T = loss to collisions   M = gain from fission multiplication

- **Define a fixed parameter k_e such that $k_e > k_0$** (k_0 = exact eigenvalue)

- **Subtract $\frac{1}{k_e}M\Psi$ from each side of the transport equation**

$$(L + T - S - \frac{1}{k_e}M)\Psi = (\frac{1}{K_{eff}} - \frac{1}{k_e})M\Psi$$

- **Solve the modified transport equation by power iteration**

$$(L + T - S - \frac{1}{k_e}M)\Psi^{(n+1)} = (\frac{1}{K_{eff}^{(n)}} - \frac{1}{k_e})M\Psi^{(n)}$$

- **Power iteration for modified transport equation**

$$(L + T - S - \frac{1}{k_e}M)\Psi^{(n+1)} = (\frac{1}{K_{eff}^{(n)}} - \frac{1}{k_e})M\Psi^{(n)}$$

$$\Psi^{(n+1)} = (\frac{1}{K_{eff}^{(n)}} - \frac{1}{k_e}) \cdot (L + T - S - \frac{1}{k_e}M)^{-1}M\Psi^{(n)}$$

$$\Psi^{(n+1)} = \frac{1}{\tilde{K}^{(n)}} \cdot \tilde{F}\Psi^{(n)}$$

$$\text{where} \quad \tilde{K}^{(n)} = (\frac{1}{K_{eff}^{(n)}} - \frac{1}{k_e})^{-1} \quad \text{or} \quad K_{eff}^{(n)} = (\frac{1}{\tilde{K}^{(n)}} + \frac{1}{k_e})^{-1}$$

- **How to choose k_e**
  - **k_e must be larger than k_0**   (but, don't know k_0!)
  - **k_e must be held constant for all of the histories in a batch, but can be adjusted between batches**
    - Typically, guess a large initial value for k_e, such as $k_e=5$ or $k_e=2$
    - Run a few batches, keeping k_e fixed, to get an initial estimate of K_{eff}
    - Adjust k_e to a value slightly larger than the estimated K_{eff}
    - Run more batches, possibly adjusting k_e if the estimated K_{eff} changes

Wielandt Method

- **Convergence**
  - Eigenfunctions for the Wielandt method are same as for basic power iteration
  - Eigenvalues are shifted:

$$\tilde{k}_J = \left[\frac{1}{k_J} - \frac{1}{k_e} \right]^{-1} \qquad\qquad k_e > k_0 > k_1 > \ldots$$

  - Expand the initial guess, substitute into Wielandt method, rearrange to:

$$\Psi^{(n+1)} \approx [\text{cons}\tan t] \cdot \left[\vec{u}_0 + \left(\frac{a_1^{(0)}}{a_0^{(0)}} \right) \cdot \left(\frac{k_e - k_0}{k_e - k_1} \cdot \frac{k_1}{k_0} \right)^{n+1} \cdot \vec{u}_1 + \ldots \right]$$

$$K^{(n+1)} \approx k_0 \cdot \left[1 + \left(\frac{a_1^{(0)}}{a_0^{(0)}} \right) \cdot \left(\frac{k_e - k_0}{k_e - k_1} \cdot \frac{k_1}{k_0} \right)^{n} \cdot \left(\frac{k_e - k_0}{k_e - k_1} \cdot \frac{k_1}{k_0} - 1 \right) \cdot G_1 + \ldots \right]$$

  - **Additional factor $(k_e\text{-}k_0)/(k_e\text{-}k_1)$ is less than 1 and positive, so that the red terms die out faster than for standard power iteration**

- The **dominance ratio** for this modified power iteration is

$$DR' = \frac{\tilde{k}_1}{\tilde{k}_0} = \frac{[\frac{1}{k_1} - \frac{1}{k_e}]^{-1}}{[\frac{1}{k_0} - \frac{1}{k_e}]^{-1}} = \frac{k_e - k_0}{k_e - k_1} \cdot \frac{k_1}{k_0} = \frac{k_e - k_0}{k_e - k_1} \cdot DR$$

  - Since $k_e > k_0$ and $k_0 > k_1$, **DR' < DR**
  - DR of Wielandt method is always **smaller** than standard power iteration

- **Wielandt acceleration improves the convergence rate of the power iteration method for solving the k-eigenvalue equation**
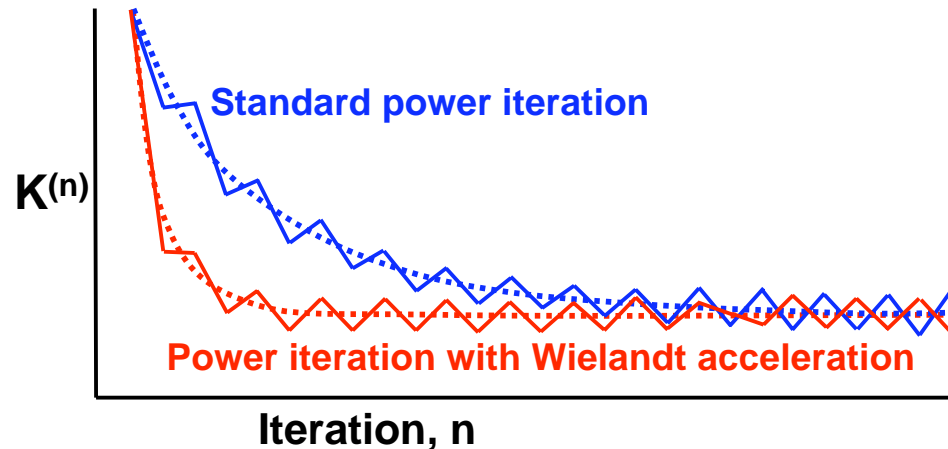
$\Rightarrow$ **Weilandt method converges at a faster rate than power iteration**

- **Monte Carlo procedure for Wielandt acceleration**

$$(L + T - S - \tfrac{1}{k_e}M)\Psi^{(n+1)} = \left(\tfrac{1}{K_{eff}^{(n)}} - \tfrac{1}{k_e}\right)M\Psi^{(n)}$$

- **For standard Monte Carlo (power iteration) in generation n+1**

  – When a collision occurs, the expected number of fission neutrons produced is

$$n_F = \left\lfloor wgt \cdot \frac{\nu\Sigma_F}{\Sigma_T} \cdot \frac{1}{K^{(n)}} + \xi \right\rfloor$$

  – **Store n_F copies of particle in the "fission bank"**

  – **Use the fission bank as the source for the next generation (n+2)**

- **For Monte Carlo Wielandt method in generation n+1**

  – When a collision occurs, compute 2 expected numbers of fission neutrons

$$n'_F = \left\lfloor wgt \cdot \frac{\nu\Sigma_F}{\Sigma_T} \cdot \left(\frac{1}{K^{(n)}} - \frac{1}{k_e}\right) + \xi \right\rfloor \qquad n'_e = \left\lfloor wgt \cdot \frac{\nu\Sigma_F}{\Sigma_T} \cdot \frac{1}{k_e} + \xi \right\rfloor$$

  – Note that $E[\, n'_F + n'_e \,] = E[\, n_F \,]$

  – **Store n'_F copies of particle in the "fission bank"**

  – **Follow n'_e copies of the particle in the current generation (n+1)**

  – **Use the fission bank as the source for the next generation (n+2)**

- **<u>Power iteration</u> for Monte Carlo k-effective calculation**

Initial Guess

Batch 1 $K_{eff}^{(1)}$

Batch 2 $K_{eff}^{(2)}$

Batch 3 $K_{eff}^{(3)}$

Batch 4 $K_{eff}^{(4)}$

Batch 1 Source

Batch 2 Source

Batch 3 Source

Batch 4 Source

Batch 5 Source

● Source particle generation

● Monte Carlo random walk

↗ Neutron
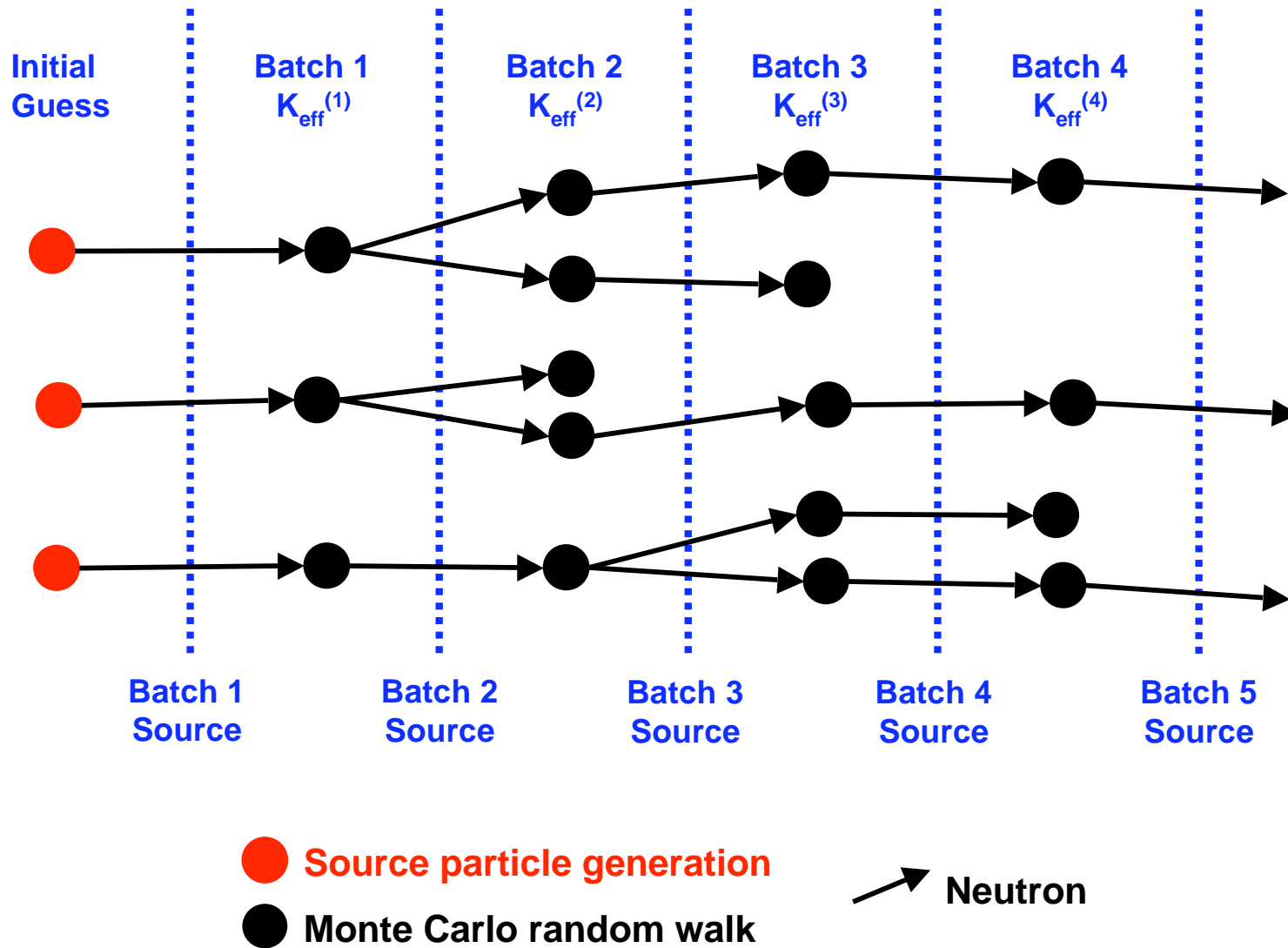
Wielandt Method

- **Wielandt method** for Monte Carlo k-effective calculation

Initial Guess | **Batch 1** $K_{eff}^{(1)}$ | **Batch 2** $K_{eff}^{(2)}$ | **Batch 3** $K_{eff}^{(3)}$ | **Batch 4** $K_{eff}^{(4)}$

Batch 1 Source | **Batch 2 Source** | **Batch 3 Source** | **Batch 4 Source** | **Batch 5 Source**
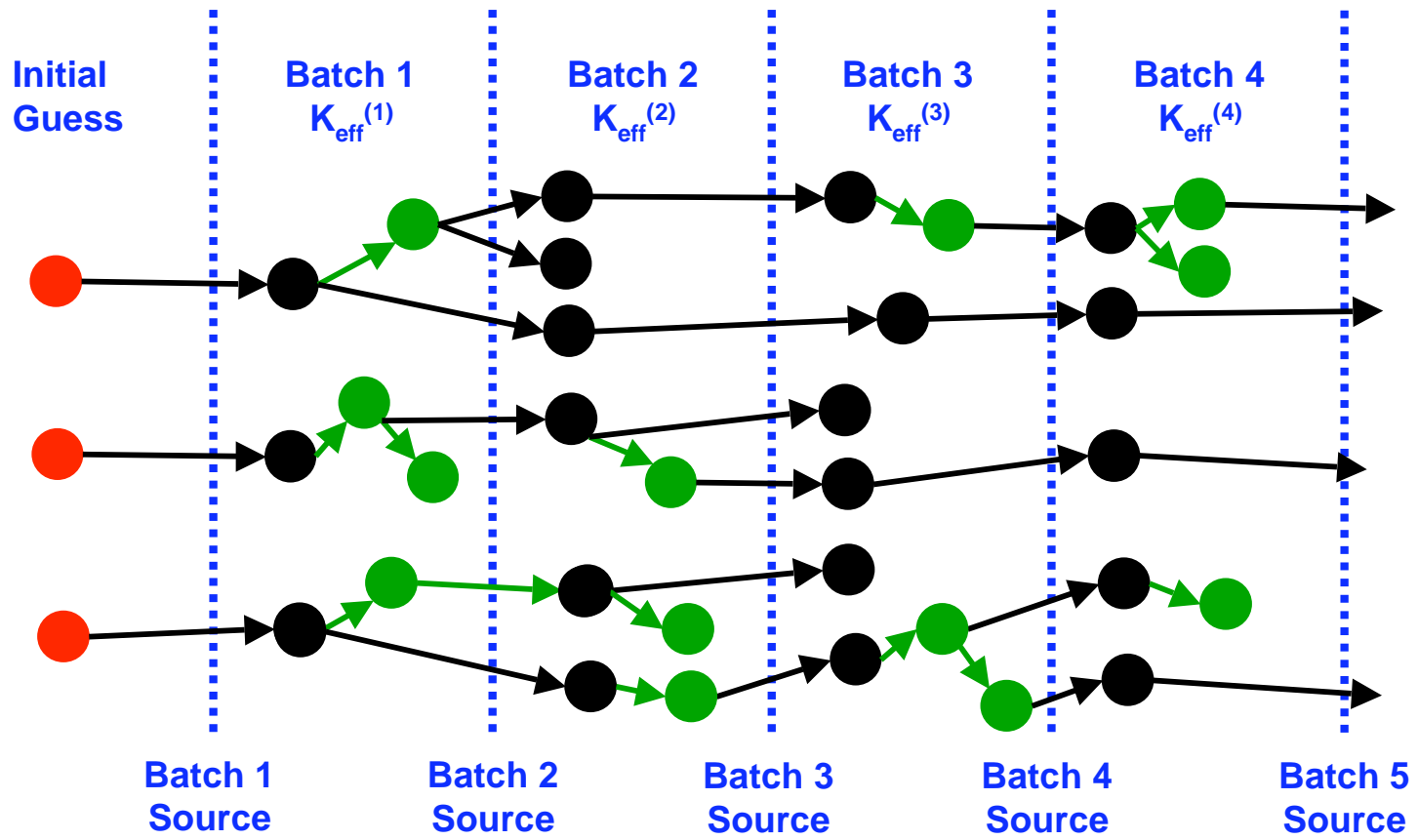
🔴 **Source particle generation**

⚫ **Monte Carlo random walk**

➚ **Neutron**

🟢 **Additional Monte Carlo random walks within generation due to Wielandt method**

Summary

- **<u>Wielandt Method has a lower DR than power iteration</u>**

    - **Faster convergence <u>rate</u> than power iteration $\Rightarrow$ fewer iterations**

    - **Some of the particle random walks are moved from the next generation into the current generation $\Rightarrow$ more work per iteration**

    - **Same total number of random walks $\Rightarrow$ no reduction in CPU time**

- **<u>Advantages</u>**

    - **Reduced chance of false convergence for very slowly converging problems**

    - **Reduced inter-generation correlation effects on variance**

    - **Fission source distribution spreads more widely in a generation (due to the additional particle random walks), which should result in more interactions for loosely-coupled problems**

- **Standard generation model, solved by power iteration**

$$\Psi^{(n+1)} = \frac{1}{K_{eff}^{(n)}} \cdot F \Psi^{(n)}$$

- **Superhistory method**

  - **Follow several generations (L) before recomputing K_{eff} and renormalizing**

$$\Psi^{(n+1)} = \frac{1}{\tilde{K}^{(n)}} \cdot \tilde{F} \Psi^{(n)}, \qquad \text{with} \quad \tilde{F} = F^L, \quad \tilde{K}^{(n)} = (K_{eff}^{(n)})^L$$

- **Convergence**

  - Same eigenfunctions as standard power iteration
  - Eigenvalues are k_0^L, k_1^L, k_2^L, …
  - $DR' = DR^L$, where DR = dominance ratio for power iteration
  - Fewer iterations, but L generations per iteration $\Rightarrow$ same work as power iteration
  - Same convergence rate as power iteration

- **Advantages**

  - Reduced correlation between iterations
  - Fewer renormalizations

- **Superhistory Method** for Monte Carlo k-effective calculation

Example with L = 2 generations/batch

Initial Guess

Batch 1 $K_{eff}^{(1)}$

Batch 2 $K_{eff}^{(4)}$

Batch 1 Source

Batch 2 Source

Batch 3 Source
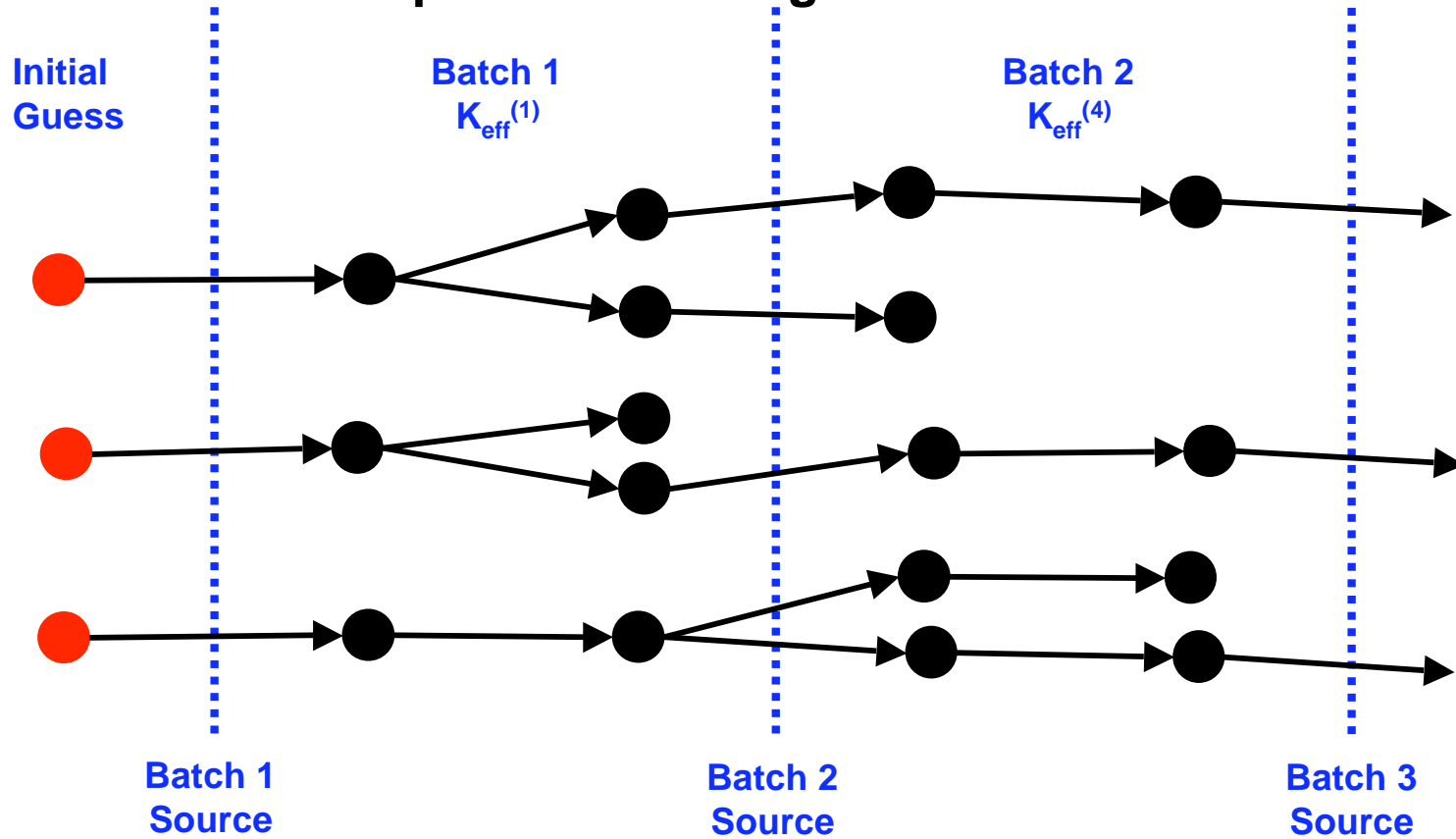
🔴 **Source particle generation**

⚫ **Monte Carlo random walk**

↗ **Neutron**

Monte Carlo k-effective Calculations

J. Lieberoth, "A Monte Carlo Technique to Solve the Static Eigenvalue Problem of the Boltzmann Transport Equation," *Nukleonik* **11**,213 (1968).

M. R. Mendelson, "Monte Carlo Criticality Calculations for Thermal Reactors," *Nucl. Sci Eng.* **32**, 319–331 (1968).

H. Rief and H. Kschwendt, "Reactor Analysis by Monte Carlo," *Nucl. Sci. Eng.*, **30**, 395 (1967).

W. Goad and R. Johnston, "A Monte Carlo Method for Criticality Problems," *Nucl. Sci. Eng.* **5**, 371–375 (1959).

Superhistory Method

R.J. Brissenden and A.R. Garlick, "Biases in the Estimation of Keff and Its Error by Monte Carlo Methods," *Ann. Nucl. Energy*, Vol 13, No. 2, 63–83 (1986).

Wielandt Method

T Yamamoto & Y Miyoshi, "Reliable Method for Fission Source Convergence of Monte Carlo Criticality Calculation with Wielandt's Method", *J. Nuc. Sci. Tech.*, **41**, No. 2, 99–107 (Feb 2004).

S Nakamura, <u>Computational Methods in Engineering and Science</u>, R. E. Krieger Pub. Company, Malabar, FL (1986).

Sandwich Method

J Yang & Y. Naito, "The Sandwich Method for Determining Source Convergence in Monte Carlo Calculations", *Proc. 7th Int. Conf. Nuclear Criticality Safety, ICNC2003, Tokai-mura, Iburaki, Japan, Oct 20–24, 2003*, JAERI-Conf 2003–019, 352 (2003).

HTGR Modeling
&
Stochastic Geometry
With MCNP5

- **Very High Temperature Gas-Cooled Reactor**
  - One of the Next Generation Nuclear Reactors
  - Average coolant temperatures above 900 C, operational fuel temperatures above 1250 C
  - Higher energy conversion efficiency
  - Thermochemical hydrogen production

- **Two types of Reactor Design**
  - **Prismatic** fuel type reactor design, with fuel "compacts"
  - **Pebble bed** fuel type reactor design
  - "Double Heterogeneity" due to the fuel kernels inside fuel compacts/pebbles in the core

Example – Very High Temperature Gas Cooled Reactor
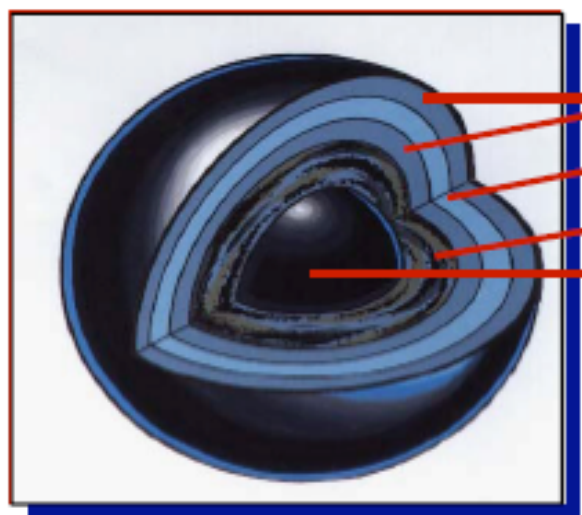
- Pyrolytic Carbon
- Silicon Carbide
- Porous Carbon Buffer
- Uranium Oxycarbide

~1 mm

TRISO Coated fuel particles (left) are formed into fuel rods (center) and inserted into graphite fuel elements (right).

PARTICLES

COMPACTS

FUEL ELEMENTS

P. E. MacDonald, et al., "NGNP Preliminary Point Design – Results of the Initial Neutronics and Thermal-Hydraulic Assessments During FY-03", INEEL/EXT-03–00870 Rev. 1, Idaho National Engineering and Environmental Laboratory (2003).

Core

Assembly

Kernel
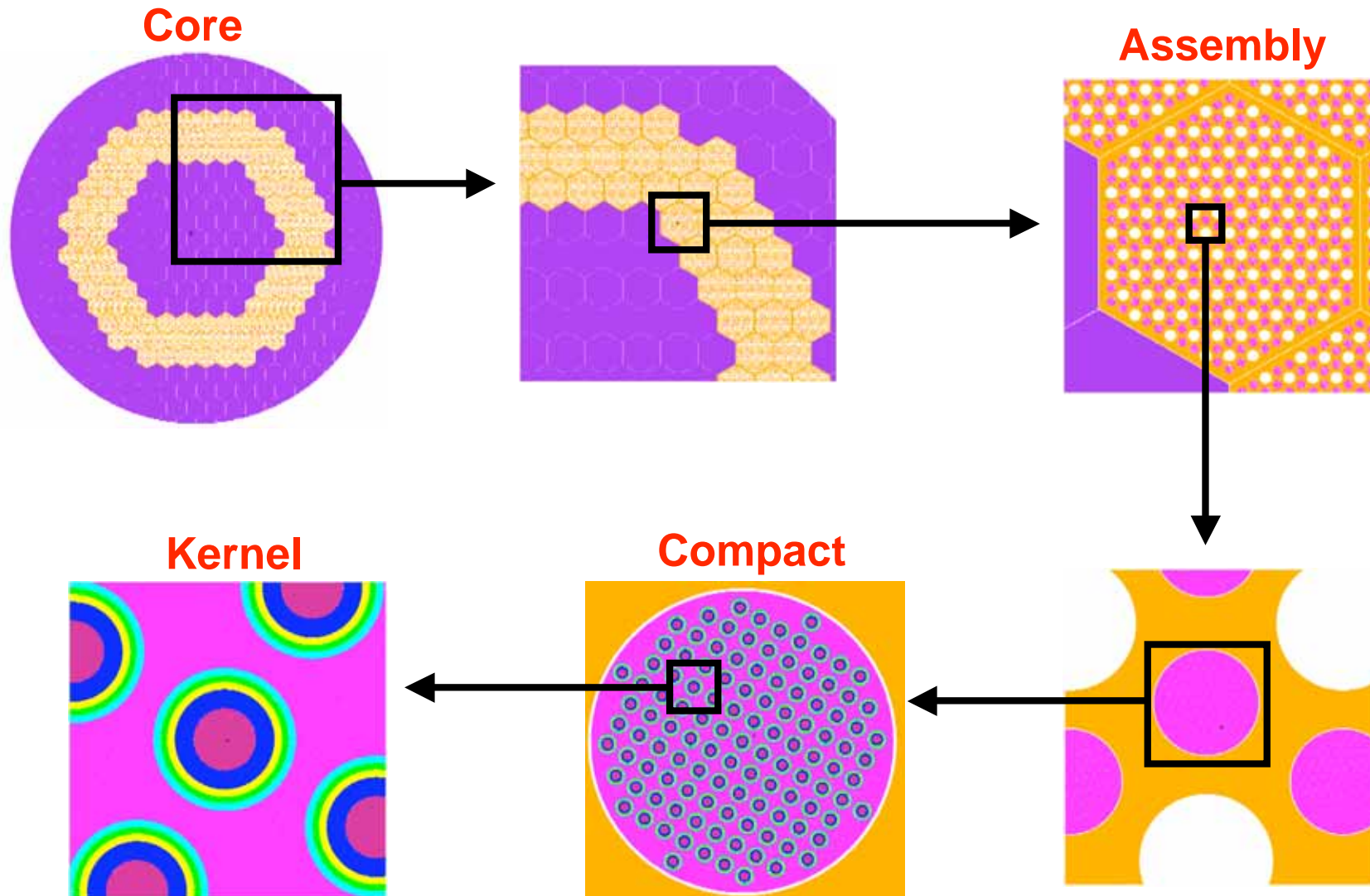
Compact

- **Existing MCNP geometry can handle:**
  - 3D description of core
  - **Fuel compacts or lattice of pebbles**
    - Typically, **hexagonal lattice** with close-packing of spherical pebbles
    - Proteus experiments: ~ 5,000 fuel pebbles
                                            ~ 2,500 moderator pebbles

  - **Lattice of fuel kernels** within compact or pebble
    - Typically, **cubic lattice** with kernel at center of lattice element
    - Proteus experiments: ~ 10,000 fuel kernels per pebble
                                            ~ 50 M   fuel kernels, total

  - Could introduce random variations in locations of a few thousand cells in MCNP input, but **not** a few million.

  - See papers by: Difilipo,   Plukiene et al, Ji-Conlin-Martin-Lee, etc.

- When a neutron enters a new lattice element, a transformation is made to the neutron's position & direction to the local coordinates of the universe embedded in that lattice element. [standard MCNP]

- **Users can flag selected universes as "stochastic"**   [new]
  - A neutron entering a lattice element containing a stochastic universe undergoes the normal transformations.

  - Then, additional **random translations** are made:

$$x \leftarrow x + (2\xi_1 - 1) \cdot \delta_x$$
$$y \leftarrow y + (2\xi_2 - 1) \cdot \delta_y$$
$$z \leftarrow z + (2\xi_3 - 1) \cdot \delta_z$$

  - Then, tracking proceeds normally, with the universe coordinates fixed until the neutron exits that lattice element

MCNP5 Stochastic Geometry

mcnp5

**Diagnostics
Applications
Group (X-5)**

Los Alamos
NATIONAL LABORATORY

- Neutron on lattice edge, about to enter embedded universe
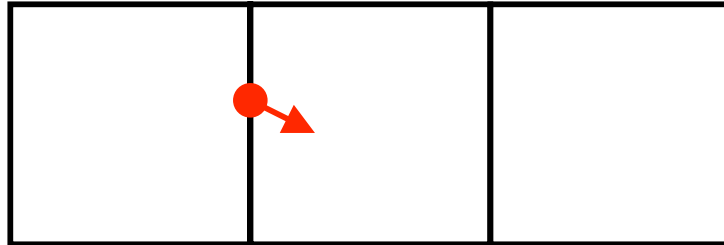
- Embedded universe,

    before random translation   **after** random translation
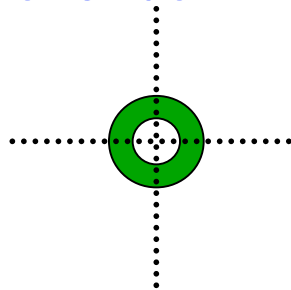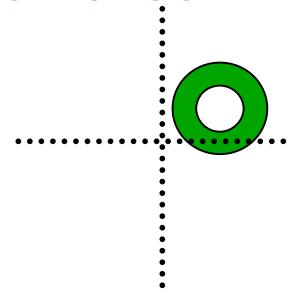
- Track normally, until neutron exits the lattice element

MCNP5 Stochastic Geometry

mcnp5

**Diagnostics
Applications
Group (X-5)**

Los Alamos
NATIONAL LABORATORY
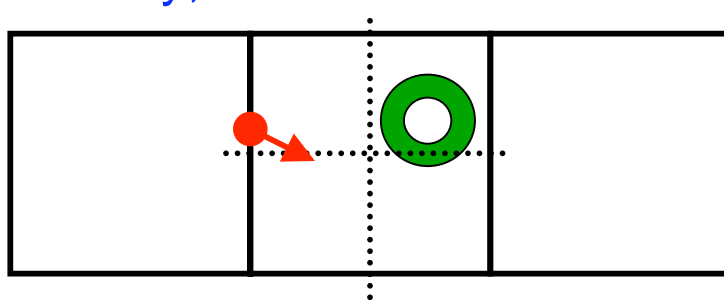
- **On-the-fly random translations of embedded universes in lattice**
  - Does not require any extra memory storage
  - Very little extra computing cost -
    only 3 random numbers for each entry into a stochastic universe

- **For K-effective calculations (KCODE problems)**
  - If fission occurred within fuel kernel, should have source site in next
    cycle be at same position within fuel kernel
  - Need to save $\delta_x, \delta_y, \delta_z$ along with neutron coordinates in fission bank
  - On source for next cycle, apply $\delta_x, \delta_y, \delta_z$ after neutron pulled from bank

- **To preserve mass exactly**, rather than on the average
  stochastically, must choose $\delta_x, \delta_y, \delta_z$ so that fuel kernels are not
  displaced out of a lattice element

maximum δ_x

Stochastic Effects
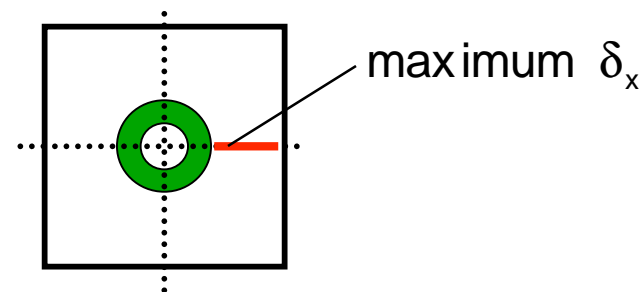
- **MCNP5 stochastic geometry**
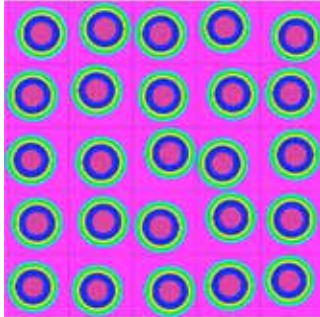
Fuel kernels displaced randomly on-the-fly within a lattice element each time that neutron enters

- **RSA placement of fuel kernels**
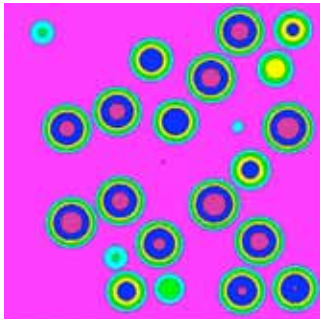
Fuel kernels placed randomly in job input, using Random Sequential Addition

Standard MCNP5 – geometry is fixed for entire calculation (Does not use stochastic geometry)

Stochastic Effects – Results

MCNP5 Results for Infinite Lattices of Fuel Kernels

Method	K-effective
Fixed 5x5x5 lattice with centered spheres	1.1531 ± 0.0004
Fixed 5x5x5 lattice with randomly located spheres ("on the fly")	1.1515 ± 0.0004
Multiple (25) realizations of 5x5x5 lattice with randomly located spheres	1.1513 ± 0.0004
Multiple (25) realizations of randomly packed (RSA) fuel "box"	1.1510 ± 0.0003

$\Rightarrow$ **Small but significant effect from stochastic geometry**

$\Rightarrow$ **New MCNP5 stochastic geometry matches multiple realizations**

$\Rightarrow$ **New MCNP5 stochastic geometry matches true random (RSA)**

- ## TRISO fuel kernels in graphite matrix
  - Fuel kernel geometry & composition taken from the NGNP Point Design (MacDonald et al. 2003)
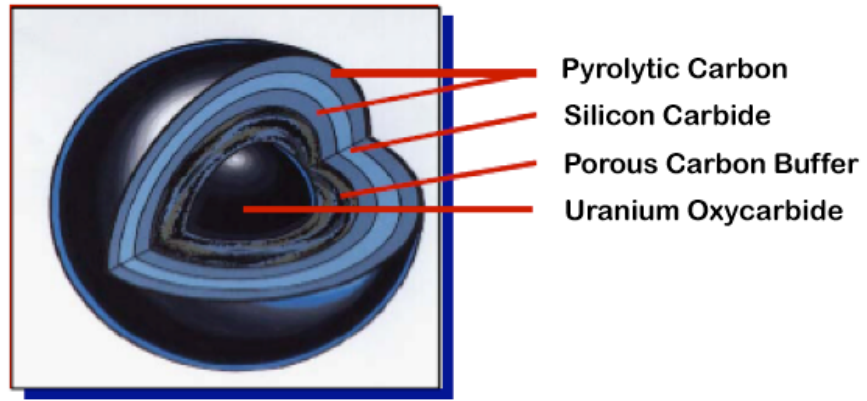
TRISO Fuel Kernel Geometry and Composition

Region #	Name	Outer radius (μ)	Composition	Density (g/cc)
1	Uranium oxycarbide	175	UCO ($UC^{.5}O^{1.5}$)	10.5
2	Porous carbon buffer	275	C	1.0
3	Inner pyrolytic carbon	315	C	1.9
4	Silicon carbide	350	SiC	3.2
5	Outer pyrolytic carbon	390	C	1.9

  - **Fuel kernel packing fraction = .289**

Fuel Kernels – Simplified Model
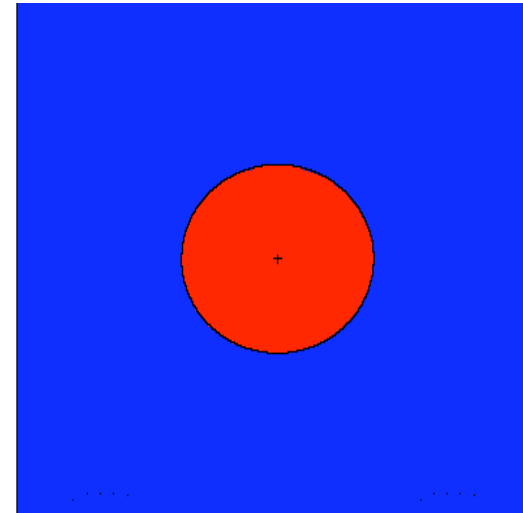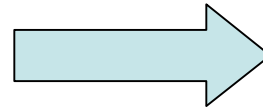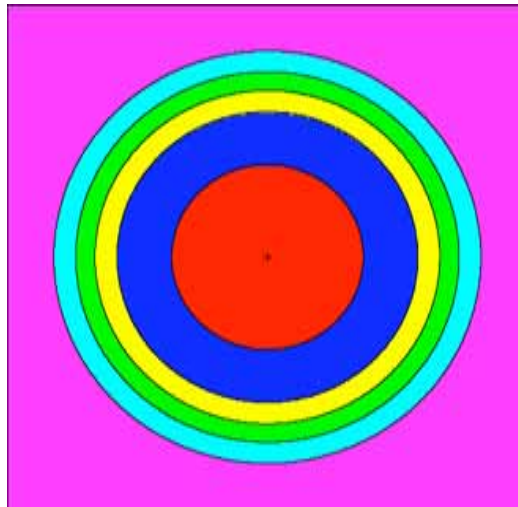
Six-region Heterogeneous

Two-Region Heterogeneous

Reflecting b.c. on all sides of cubes

MCNP5 Simulations of Fuel Kernels

Configuration	Kernel location	keff	std dev
Homogeneous microsphere cell	- – -	1.0995	.0004
Two-region heterogeneous microsphere cell	Centered	1.1535	.0004
Six-region heterogeneous microsphere cell	Centered	1.1533	.0003

⇒ **Essential to model the microsphere heterogeneity**

⇒ **Homogenizing the coatings into the matrix does not introduce any significant errors, & can reduce model complexity**

⇒ **Adequate to explicitly represent just the UCO spheres**
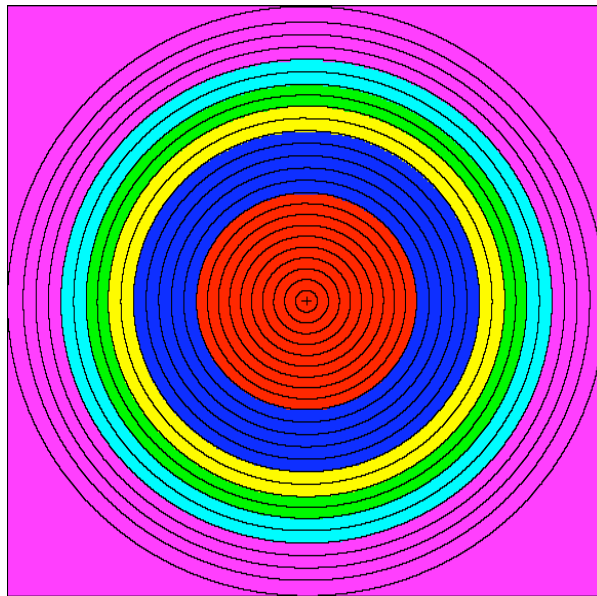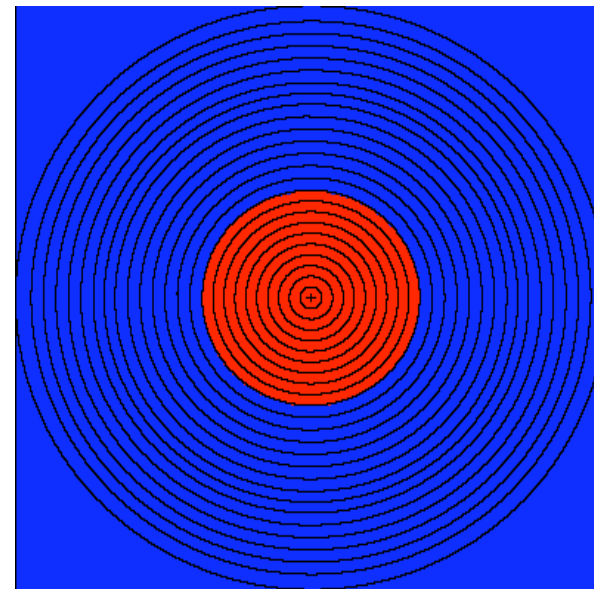
Six-Region Heterogeneous

Two-Region Heterogeneous

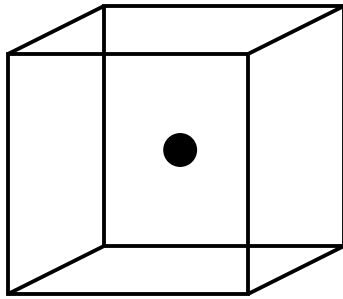**Reflecting b.c. on all sides of cubes**

mcnp5
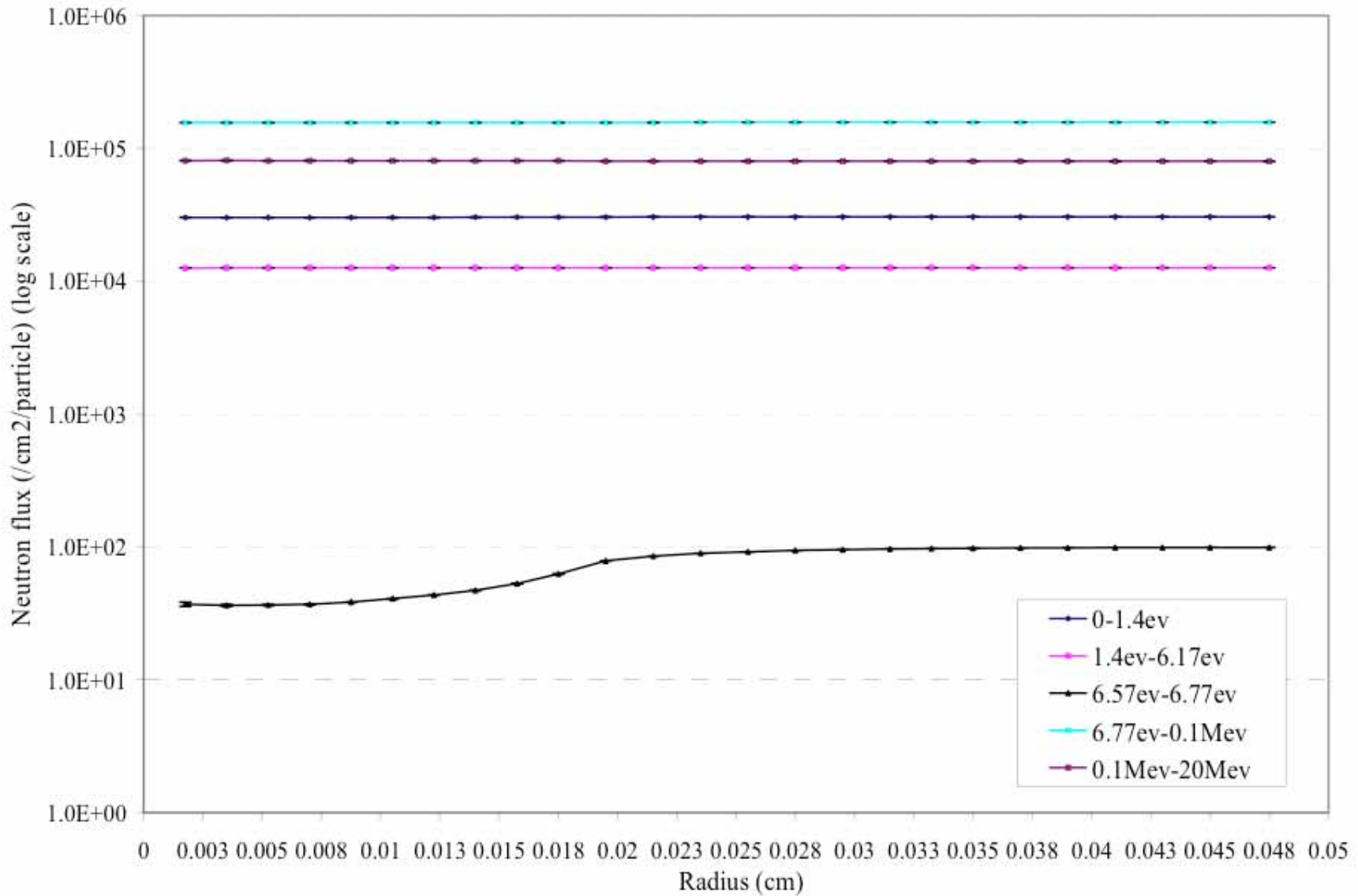
Radial Neutron Flux in Resonance Range

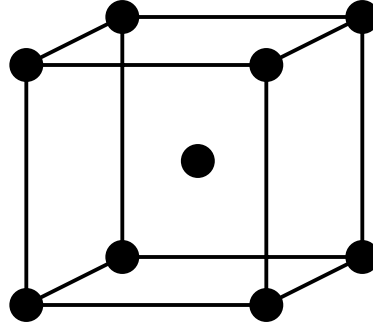- **Resonance Energy Range: 6.57eV – 6.77eV**
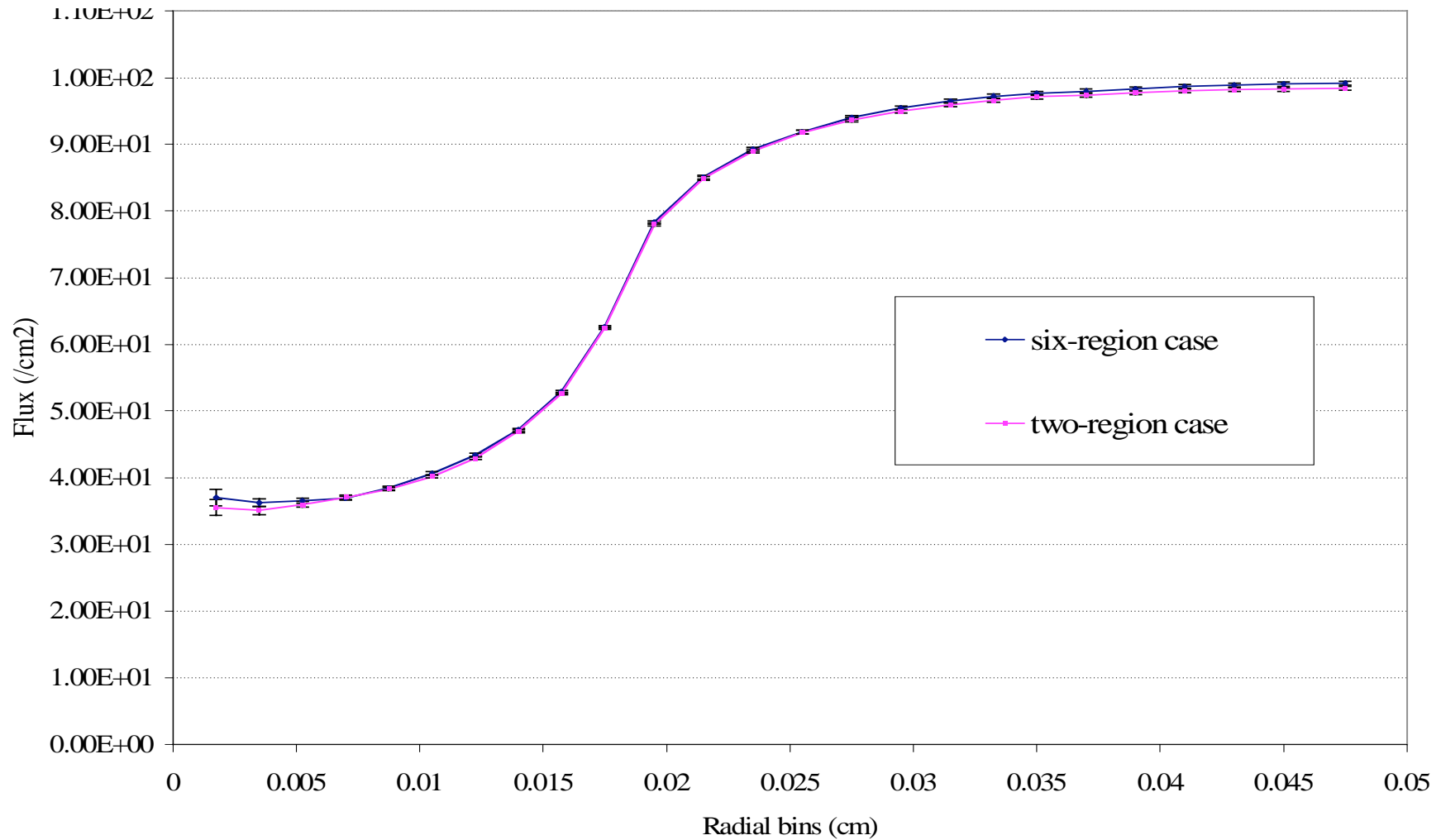
Fuel Kernel Modeling – Lattices

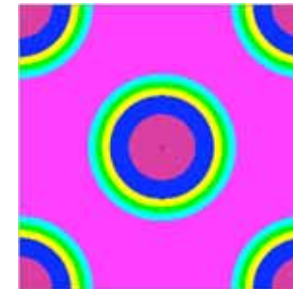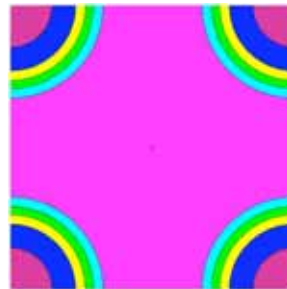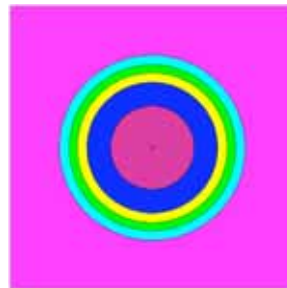| Simple cubic	Body Centered Cubic	Face Centered Cubic
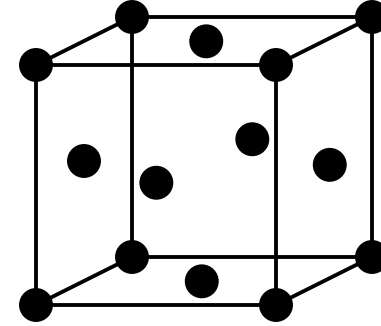
Slice through base plane

Slice through mid plane

0.09501 cm	0.119705 cm	0.150819 cm
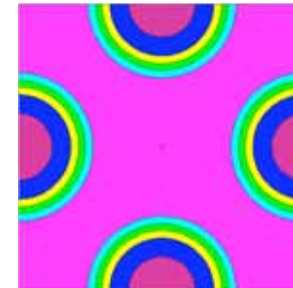
Fuel Kernel Modeling – Results

- **MCNP5 calculations for infinite geometry, fuel kernels in graphite matrix**

Configuration	K-effective $\pm\ 1\sigma$
Homogenized matrix & fuel kernel	**1.0996 ± .0008**
Simple cubic lattice pitch = 0.09501 cm	**1.1531 ± .0004**
Body centered cubic lattice pitch = 0.119705 cm	**1.1534 ± .0003**
Face centered cubic lattice pitch = 0.150819 cm	**1.1526 ± .0003**

$\Rightarrow$ **Large errors for homogenized model**

$\Rightarrow$ **Essentially same results for all lattice models**

Compact or Pebble Modeling

- **If an <u>infinite</u> lattice of fuel kernels is embedded in a compact or pebble, clipping by the enclosing cylinder or sphere results in fragments of kernels. This is not correct modeling**

- **A <u>finite</u> lattice of fuel kernels should be used, so that there are no fragments. Vertical pitch of the lattice should be adjusted to preserve total mass or packing fraction.**
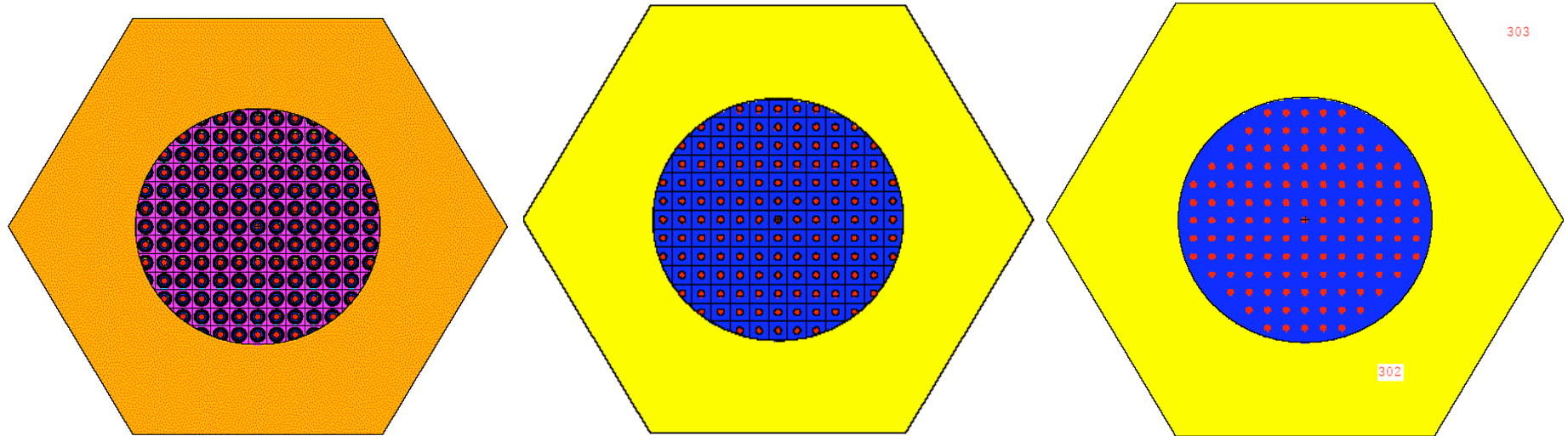
HTGR Fuel Compact
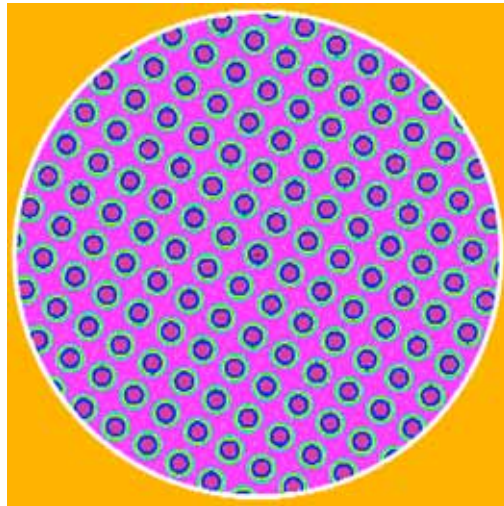
Infinite lattice of kernels, truncated by cylinder
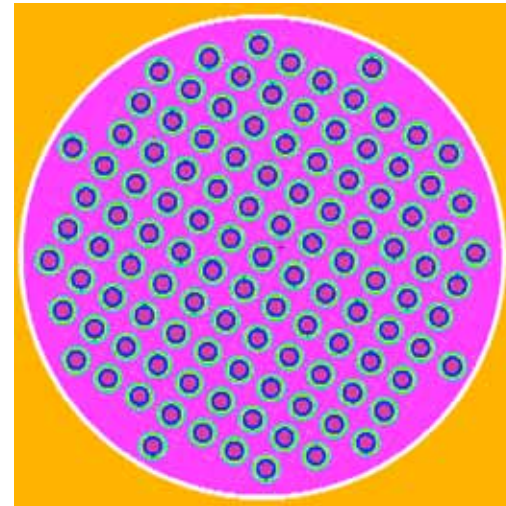
Finite lattice of kernels, no intersections with cylinder

Fuel Compacts – Graphite with Fuel Kernels

Six-region Heterogeneous (clipped)

Two-Region Heterogeneous (clipped)

Two-Region Heterogeneous (unclipped)

Reflecting b.c. on all surfaces of fuel compact cell

MCNP5 Simulations of Fuel Compact Cells

fuel compact	keff*	std dev
Homogenized fuel kernels	**1.2885**	**.0004**
Six-region centered fuel kernels (clipped)	**1.3401**	**.0004**
Six-region centered fuel kernels (not clipped)$_{.24\%\Delta\rho}$	**1.3445**	**.0002**
Two-region centered fuel kernels (not clipped)$_{.22\%\Delta\rho}$	**1.3447**	**.0002**

$\Rightarrow$ **Homogenizing the fuel kernel coatings into the graphite matrix is a reasonable approximation – saves significant computer time and simplifies input**

$\Rightarrow$ **Correct modeling of compacts, using a finite lattice to avoid partial kernels at boundary, is important**

- Homogenized core
- Homogenized compacts, heterogeneous core
- Heterogeneous core, explicit fuel kernel lattice

Case	Configuration	K-effective $\pm$ 1σ
A	Fully homogenized core	1.0155 $\pm$ .0004
B	Heterogenous core, with homogenized fuel kernels & matrix in fuel cylinders	1.0583 $\pm$ .0004
F	Heterogeneous core, with simple cubic fixed finite lattice (with no partial kernels at cylinder boundary)	1.0974 $\pm$ .0002

$\Rightarrow$ **Homogenization is so bad, it should <u>never</u> be used for HTGRs**

- Heterogeneous core, with simple cubic **infinite** lattice of kernels
  (**with partial kernels** at cylinder boundary)

- Heterogeneous core, with simple cubic **finite** lattice of kernels
  (**with no partial kernels** at cylinder boundary)

Case	Configuration	K-effective ± 1σ
E	Heterogeneous core, with simple cubic fixed <u>infinite</u> lattice (with partial kernels at cylinder boundary)	1.0948 ± .0002
F	Heterogeneous core, with simple cubic fixed <u>finite</u> lattice (with <u>no</u> partial kernels at cylinder boundary)	1.0974 ± .0002

⇒ **Correct modeling of compacts, using a finite lattice to avoid partial kernels at boundary, is important**

Full-core Calculations

- Heterogeneous core, simple cubic infinite lattice

- Heterogeneous core, simple cubic infinite lattice, with new MCNP5 **stochastic** geometry

Case	Configuration	K-effective ± 1σ
F	**Heterogeneous core, with simple cubic fixed finite lattice (with no partial kernels at cylinder boundary)**	**1.0974 ± .0002**
G	**New MCNP5 stochastic geometry, on-the-fly random location of kernels within simple cubic finite lattice elements (with no partial kernels at cylinder boundary)**	**1.0968 ± .0002**

⇒ **Stochastic effects are small for full-core calculations, may or may not be important**

Conclusions

- **The new stochastic geometry treatment for MCNP5 provides an accurate and effective means of modeling the particle heterogeneity in TRISOL particle fuel**
  - **Same results as (brute-force) multiple realizations of random geometry input with standard MCNP**
  - **Negligible difference from "truly random" multiple realizations**

- **The results indicate that:**
  - **Homogenizing the fuel or core introduces very large errors (~8%)**
  - **Double heterogeneity important only in resonance energy range**
    - Increased resonance self-shielding due the neighboring particles, so this is "particle shadowing". The effect may be explained as an increase in the Dancoff factor
    - The effect is more pronounced at fuel kernel or compact calculations, and decreases as one goes to full core due to increased moderation hence decreased effect of resonance absorption
  - **The neutronic effect of using a fixed lattice is negligible**
  - **The effect of choosing either centered spheres or randomly located spheres is small**
  - **Can introduce significant errors by using an infinite lattice truncated by compact or pebble (clipped), rather than a finite lattice**
  - **Homogenizing the fuel coatings into the graphite matrix is a reasonable approximation**

- W. Ji, J.L. Conlin, G. Yesilyurt, W.R. Martin, J.C. Lee, and F.B. Brown, "Neutronic Analysis to Support Validation of Safety Analysis Codes for the VHTR", *Trans. Am. Nucl. Soc.* **93** (Nov 2005)

- Wei Ji, J.L. Conlin, W.R. Martin, J.C. Lee, and F.B. Brown, "Explicit Modeling of Particle Fuel for the Very-High Temperature Gas-Cooled Reactor", *Trans. Am. Nucl. Soc.* **92** (June, 2005)

- F.B. Brown, W.R. Martin, W. Ji, J.L. Conlin, & J.C. Lee, "Stochastic Geometry and HTGR Modeling for MCNP5", ANS Monte Carlo 2005 Topical Meeting, Chattanooga TN, April 17–21, 2005 (April, 2005).

- W. Ji, J. Conlin, W.R. Martin, and J.C. Lee, "Reactor Physics Analysis of the VHTGR Core," *Trans. Am. Nucl.Soc.* **91**, 171–173 (Nov. 2004).

- P.E. MacDonald, et al., "NGNP Preliminary Point Design – Results of the Initial Neutronics and Thermal-Hydraulic Assessments During FY-03," INEEL/EXT-03–00870 Rev. 1. Idaho National Engineering and Environmental Laboratory (2003).

- F.C. Difilippo, "Monte Carlo Calculations of Pebble Bed Benchmark Configurations of the PROTEUS Facility," *Nucl. Sci. Eng.* **143**, 240–253 (2003).

- R. Plukiene and D. Ridikas, "Modelling of HTRs with Monte Carlo: from a homogeneous to an exact heterogeneous core with microparticles," *Annals of Nuclear Energy* **30**, 1573–1585 (2003).

- I. Murata, T. Mori, and M. Nakagawa, "Continuous Energy Monte Carlo Calculations of Randomly Distributed Spherical Fuels in High-Temperature Gas-Cooled Reactors Based on a Statistical Geometry Model," *Nucl. Sci. Eng.* **123**, 96–109 (1996).

- M. Armishaw, N. Smith, and E. Shuttlesworth, E., "Particle Packing Considerations for Pebble Bed Fuel Systems," *Proc. ICNC 2003 Conference, JAERI-Conf-2003–019, Tokai-mura, Japan* (2003).

- Z. Karriem, C. Stoker, and F. Reitsma, "MCNP Modeling of HTGR Pebble-Type Fuel," *Proc. Monte Carlo 2000 Conference*, Lisbon, 841–846 (2000).

- S. Widom, "Random Sequential Addition of Hard Spheres to a Volume," *J. Chem. Phy.* **44**, 3888-3894 (1966).